Solving Schrödinger equation in semiclassical regime with highly oscillatory time-dependent potentials

Arieh Iserles,* Karolina Kropielnicka† & Pranav Singh‡

October 12, 2018

AMS Mathematics Subject Classification: Primary 65M70, Secondary 35Q41, 65L05, 65F60

Keywords: Schrödinger equation, time dependent potentials, semiclassical regime, highly oscillatory potentials, large time steps, integral preservation, simplified commutators, Magnus expansion, symmetric Zassenhaus splittings, Lanczos iterations

Abstract

Schrödinger equations with time-dependent potentials are of central importance in quantum physics and theoretical chemistry, where they aid in the simulation and design of systems and processes at atomic and molecular scales. Numerical approximation of these equations is particularly difficult in the semiclassical regime because of the highly oscillatory nature of solution. Highly oscillatory potentials such as lasers compound these difficulties even further. Altogether, these effects render a large number of standard numerical methods less effective in this setting. In this paper we will develop a class of exponential splitting schemes that allow us to use large time steps in our schemes even in the presence of highly oscillatory potentials and solutions. These are derived by combining the advantages of integral-preserving simplified-commutator Magnus expansions with those of symmetric Zassenhaus splittings. The efficacy of these methods is demonstrated through 1D, 2D and 3D numerical examples.

*Department of Applied Mathematics and Theoretical Physics, University of Cambridge, Wilberforce Rd, Cambridge CB3 0WA, UK.

†Institute of Mathematics, Polish Academy of Sciences, 8 Śniadeckich Street, 00-656 Warsaw, Poland.

‡Mathematical Institute, Andrew Wiles Building, University of Oxford, Radcliffe Observatory Quarter, Woodstock Rd, Oxford OX2 6GG, UK and Trinity College, University of Oxford, Broad Street, Oxford OX1 3BH, UK.

1 Introduction

The Schrödinger equation in the semiclassical regime with a time-dependent electric field is the initial value problem,

$$\partial_t u(\mathbf{x},t) = \mathrm{i}\varepsilon\Delta u(\mathbf{x},t) - \mathrm{i}\varepsilon^{-1}V(\mathbf{x},t)\,u(\mathbf{x},t), \quad \mathbf{x}\in I\subseteq\mathbb{R}^d,\ t\geq 0, \tag{1.1}$$

with the initial condition $u(\mathbf{x},0)=u_0(\mathbf{x})$. Here V is a real-valued, time-dependent electric field and $0<\varepsilon\ll 1$ is the *semiclassical* parameter whose small size induces rapid oscillations of solution which cause obvious difficulties with numerical discretisation. The regularity that we require in the potential and the solution varies with the accuracy of a specific method (in the family of high-accuracy methods that we will introduce here). For the sake of simplicity, however, we assume that they are sufficiently smooth – $V(\cdot,t)\in \mathrm{C}_p^\infty(I;\mathbb{R})$ and $u(\cdot,t)\in \mathrm{C}_p^\infty(I;\mathbb{C})$. As usual, the Laplacian is $\Delta=\sum_{j=1}^d \partial_{x_j}^2$ or, for short, $\Delta=\sum_{j=1}^d \partial_j^2$.

Effective numerical approximation of this fundamental equation of quantum mechanics is of great importance and presents many computational challenges. Among the more challenging applications, for instance, is optimal control of a quantum system whose dynamics are governed by (1.1). This is the inverse problem of determining a time-dependent electric field or laser $V(\mathbf{x},t)$ that steers the initial system of underlying particles to a desired state. In practice, this involves solving a variational problem which, in turn, requires repeated numerical approximations of forward and backward equations of the form (1.1) in conjunction with an optimisation algorithm.

Such applications naturally require highly accurate but computationally inexpensive numerical methods. A wide range of highly effective methods has, indeed, been developed for solving the Schrödinger equation with time-dependent potentials, a very active research problem in theoretical chemistry, quantum physics and numerical mathematics (Tal-Ezer, Kosloff & Cerjan 1992, Peskin, Kosloff & Moiseyev 1994, Sanz-Serna & Portillo 1996, Tremblay & Carrington Jr. 2004, Ndong, Tal-Ezer, Kosloff & Koch 2010, Alvermann & Fehske 2011, Blanes, Casas & Murua 2017*a*, Blanes, Casas & Thalhammer 2017*b*, Schaefer, Tal-Ezer & Kosloff 2017, Iserles, Kropielnicka & Singh 2018).

In the setting under consideration, however, the complexity of the task is compounded due to two factors. First of all, the oscillatory nature of the solution in quantum mechanics is significantly more pronounced in the semiclassical regime. Secondly, these applications often involve potentials that feature high temporal oscillations (such as lasers).

Lanczos-based methods, e.g. (Iserles et al. 2018), are very effective in the atomic regime characterised by $\varepsilon=1$, less so in the semiclassical regime where $\varepsilon\ll 1$. Although they can still be applied in this context, they become computationally expensive. This happens because the superlinear accuracy, the most welcome feature of Krylov subspace methods such as Lanczos iterations, commences only once the number of iterations has exceeded the spectral radius of the exponent,[1] which grows like $\mathcal{O}\left(h\varepsilon^{-1}\right)$ in the semiclassical regime. Effectively, this forces us to use either a

[1] To be more precise, the number of Lanczos iterations needs to exceed half the length of the interval over which the eigenvalues of the skew-Hermitian exponent are spread (Hochbruck & Lubich 1997).

large number of Lanczos iterations or a severe depression of the time step, h, to attain sufficient accuracy. In either case, the cost grows prohibitively.

This growth of the exponent is due to the $\mathcal{O}(\varepsilon)$ wavelength spatio-temporal oscillations that appear in the solution of this equation regardless of the smoothness of the initial conditions (Bao, Jin & Markowich 2002, Jin, Markowich & Sparber 2011, Singh 2017). In order to correctly resolve these oscillations, we require

$$N = \mathcal{O}\left(\varepsilon^{-1}\right) \tag{1.2}$$

grid points in each direction in the spatial discretisation (Bao et al. 2002), causing the discretisation[2] of $\mathrm{i}\varepsilon\Delta$ to scale as $\mathcal{O}\left(\varepsilon^{-1}\right)$ since

$$\partial_j^k \rightsquigarrow \mathcal{K}_{j,k} = \mathcal{O}\left(N^k\right) = \mathcal{O}\left(\varepsilon^{-k}\right). \tag{1.3}$$

It is known that straightforward tensorisation for spatial discretisation starts becoming infeasible in dimensions higher than three. This becomes even more prohibitive when the solution is highly oscillatory, as happens in the semiclassical regime. High-dimensionality in the semiclassical regime, therefore, remains a significant challenge, even when the potential is not time-dependent.

On the other hand, even the one-dimensional case is far from trivial in the presence of a rapidly-oscillating time-dependent potential and highly oscillatory solution due to a small semiclassical parameter. These have important real-world applications in the dynamics of diatomic molecules, for instance, where x is taken to be the internuclear separation. An extremely efficient method, allowing the use of large time steps, is desired when the temporal domain is large and in applications where the solution needs to be computed repeatedly, such as in optimal control and parameter sweep applications. In (Agueny, Chovancova, Hansen & Kocbach 2016), for instance, the authors consider a parameter sweep for a one-dimensional problem with spatial and temporal domains of size 10^5, each.

Recently a specialized approach for semiclassical regime was developed in (Bader, Iserles, Kropielnicka & Singh 2014) and (Bader, Iserles, Kropielnicka & Singh 2016). In (Bader et al. 2014) a new methodology of *symmetric Zassenhauss splitting* was introduced for effectively treating the case of time-independent potentials. This splitting was termed an *asymptotic* splitting due to the manner in which it separates vastly differing scales, enabling far cheaper computation of exponentials in the semiclassical regime. In (Bader et al. 2016) we extended this approach to the case of time-dependent potentials in semiclassical regime by applying the symmetric Zassenhaus splitting algorithm (see Appendix B) to the Magnus expansion (Blanes, Casas, Oteo & Ros 2009, Iserles, Munthe-Kaas, Nørsett & Zanna 2000) and using ideas pioneered in (Munthe-Kaas & Owren 1999). Since this approach commences from a Magnus expansion where the integrals are discretised at the outset, however, it can be ineffective in the case of highly oscillatory potentials.

[2]Throughout this manuscript we use arrow $\rightsquigarrow$ in $\mathcal{L} \rightsquigarrow L$ to denote spatial discretisation of an operator $\mathcal{L}$ by the matrix L.

1.1 The approach of this paper

In this paper we develop an effective computational approach for Schrödinger equations in semiclassical regime featuring time-dependent potentials that may be highly oscillatory. These methods are based on high-order Magnus expansions and symmetric Zassenhaus splittings. The purpose, however, is not necessarily to derive schemes that are high-order in h, but those which allow the use of large time steps in order to provide accurate solutions at reasonable costs despite the presence of rapid oscillations in the solution and the potential. Our schemes work effectively for time steps that may span multiple oscillations of the time-dependent potential, for instance, as well as time steps as large as $h = \mathcal{O}(\sqrt{\varepsilon})$, spanning multiple oscillations of the solution $u(\mathbf{x}, t)$, which features temporal oscillations of wavelength $\mathcal{O}(\varepsilon)$.

In order to develop these efficient schemes, we do not analyse accuracy merely in terms of the time step, h, but also take into account the small parameter ε and the growth of the spectral radius due to a fine spatial resolution (which are typically hidden and appear as large error constants and large cost of Lanczos iterations). Following the strategy of (Bader et al. 2014), we establish the relation

$$h = \mathcal{O}(\varepsilon^{\sigma}), \ \sigma \geq 0, \quad N = \mathcal{O}\left(\varepsilon^{-1}\right),$$

and analyse the accuracy in terms of ε. In particular, we seek methods that work effectively for $\sigma < 1$, such as $\sigma = \frac{1}{2}$.

The approach proposed here allows us to develop methods of arbitrarily high accuracy in arbitrary number of dimensions (within the constraints of effective spatial discretisation). We choose optimal tools for this purpose, introducing new ones where required for further efficiency. In particular:

1. We start the derivation of our schemes from the integral-preserving simplified-commutator Magnus expansions of (Iserles et al. 2018).

2. Instead of directly resorting to Lanczos iterations for exponentiating the Magnus expansion (which proves to be a costly approach in the semiclassical regime), we perform a symmetric Zassenhaus splitting on this Magnus expansion. The use of this asymptotic splitting algorithm separates scales. Consequently, only very small exponents (in terms of spectral radius) need be exponentiated via Lanczos iterations. This enables a far cheaper computation of exponentials.

3. Lastly, we introduce a technique to lower the number of exponentials by carefully exploiting the time-symmetry of Magnus expansions. This involves starting from a slightly modified version of the Magnus expansions of (Iserles et al. 2018), which will be expressed solely in odd powers of the time step.

1.2 The first two Magnus–Zassenhaus splittings

The simplest method in the family of methods introduced in this paper is the splitting

$$\boldsymbol{u}^1 = \mathrm{e}^{\frac{1}{2}\mathrm{i}h\varepsilon\sum_{j=1}^{d}\mathcal{K}_{j,2}}\mathrm{e}^{-\mathrm{i}\varepsilon^{-1}\mathcal{D}_{\mu_{0,0}(h)}}\mathrm{e}^{\frac{1}{2}\mathrm{i}h\varepsilon\sum_{j=1}^{d}\mathcal{K}_{j,2}}\boldsymbol{u}^0 \tag{1.4}$$

where, under spectral collocation as a choice of spatial discretisation, $\mathcal{K}_{j,k}$ is a discretisation of ∂_j^k, $\mathcal{D}_f$ is the diagonal matrix with values of f along the diagonal, and

$\mu_{0,0}(h) = \int_0^h V(\xi)d\xi$. The approximation of $\mu_{0,0}(h)$ at the midpoint by $hV(h/2)$, reminiscent of the familiar *Strang splitting,* results in the so-called *exponential midpoint rule* with $\mathcal{O}\left(h^3\right)$ local error[3], which is well known and has been in use for a long while (Lubich 2008).

The first non-trivial splitting in the family of Magnus–Zassenhaus splittings introduced in this paper is the splitting

$$\boldsymbol{u}^1 = \mathrm{e}^{\frac{1}{2}\mathrm{i}h\varepsilon\sum_{j=1}^d \mathcal{K}_{j,2}}\mathrm{e}^{-\frac{1}{2}\mathrm{i}\varepsilon^{-1}\mathcal{D}_{\mu_{0,0}(h)}}\mathrm{e}^{\mathcal{W}}\mathrm{e}^{-\frac{1}{2}\mathrm{i}\varepsilon^{-1}\mathcal{D}_{\mu_{0,0}(h)}}\mathrm{e}^{\frac{1}{2}\mathrm{i}h\varepsilon\sum_{j=1}^d \mathcal{K}_{j,2}}\boldsymbol{u}^0, \tag{1.5}$$

where $\mu_{1,1}(h) = \int_0^h (\xi - h/2)V(\xi)d\xi$ and the central exponent is

$$\begin{aligned}\mathcal{W} = \sum_{j=1}^d \Big[&\tfrac{1}{6}\mathrm{i}h\varepsilon^{-1}\mathcal{D}_{(\partial_j\mu_{0,0}(h))^2} + \left(\mathcal{K}_{j,1}\mathcal{D}_{\partial_j\mu_{1,1}(h)} + \mathcal{D}_{\partial_j\mu_{1,1}(h)}\mathcal{K}_{j,1}\right)\\ &-\tfrac{1}{12}\mathrm{i}h^2\varepsilon\left(\mathcal{K}_{j,2}\mathcal{D}_{\partial_j^2\mu_{0,0}(h)} + \mathcal{D}_{\partial_j^2\mu_{0,0}(h)}\mathcal{K}_{j,2}\right)\Big]\\ &+\tfrac{1}{6}\mathrm{i}h^2\varepsilon\sum_{i=1}^{d-1}\sum_{j=i+1}^{d}\left(\mathcal{D}_{\partial_i\partial_j\mu_{0,0}(h)}\mathcal{K}_{i,1}\mathcal{K}_{j,1} + \mathcal{K}_{i,1}\mathcal{K}_{j,1}\mathcal{D}_{\partial_i\partial_j\mu_{0,0}(h)}\right),\end{aligned}$$

which will be derived in Section 2.

Remark 1 *While (1.5) is derived using fourth-order expansions, it is not a fourth-order scheme in the traditional sense (i.e. in terms of h). Instead, as mentioned previously, we analyse the accuracy in powers of ε after taking into account ε, h and the spectral growth due to spatial resolution. The global accuracy of (1.5) in term of ε is $\mathcal{O}\left(\varepsilon^{4\sigma-1}\right)$. Thus, it is an order $4\sigma - 1$ method in ε. For the sake of brevity, however, we will call it a fourth-order 'based' method.*

1.3 Organisation of the paper

Section 2 is devoted to the derivation of (1.5), our first non-trivial scheme for (1.1) which is based on a fourth-order expansion. Subsection 2.1 starts with a straightforward rewriting of the fourth-order integral-preserving simplified-commutator Magnus expansion of (Iserles et al. 2018) in the semiclassical regime. An analysis of the size of various terms is carried out in Subsection 2.2, while keeping discretisation considerations in mind, followed by a symmetric Zassenhaus splitting in Subsection 2.3. Implementation details for this scheme are discussed briefly in Subsection 2.4. For the sake of clarity, subsections 2.1–2.4 are concerned with the one-dimensional case ($d = 1$), while the complete method for arbitrary d is presented in subsection 2.5.

The derivation of the sixth-order based Magnus–Zassenhaus scheme of Section 3 is more involved than the approach in Section 2 and will only be presented in the one-dimensional case. In contrast to the fourth-order Magnus expansion, the sixth

[3] In the context of our Magnus expansions, which are *power-truncated*, time-symmetric and consequently feature only odd powers in the Taylor expansion, any $\mathcal{O}\left(h^{2k}\right)$ quadrature method automatically becomes $\mathcal{O}\left(h^{2k+1}\right)$. In particular, evaluation at middle of the interval incurs $\mathcal{O}\left(h^3\right)$ error. See (Iserles et al. 2018) for a more detailed narrative.

and higher order Magnus expansions of (Iserles et al. 2018) feature even powers of the time step. In Subsection 3.2 we discuss how these even powers result in a large number of exponential stages. An approach for remedying this issue, which involves expressing the Magnus expansion solely in odd powers of the time step, is developed in Subsections 3.3–3.6. We conclude the derivation by performing a Zassenhaus splitting on such a modified Magnus expansion in Subsection 3.7.

Numerical examples confirming the efficiency of our schemes are provided in Section 4, where we present the results obtained with our fourth-order based method for $d = 3$ and sixth-order based method for $d = 1$. In the last section, we briefly summarise the main conclusions.

The rules for simplifying commutators from (Singh 2015) and the symmetric Zassenhaus algorithm of (Bader et al. 2014), which are both utilised in the derivation of the Zassenhaus splitting in Subsections 2.3 and 3.7, are confined to Appendices A and B, respectively.

2 Fourth-order based Magnus–Zassenhaus splitting

Following the approach of (Bader et al. 2016, Iserles et al. 2018), the Schrödinger equation (1.1) can be written in the form

$$u'(t) = A(t)u(t), \qquad t \geq 0, \tag{2.1}$$

with $A(t) = \mathrm{i}[\varepsilon\Delta - \varepsilon^{-1}V(t)]$. Its solution can be approximated via the Magnus expansion (Magnus 1954), which is an infinite series of nested integrals and commutators. In practice we use finite truncations of this series for a numerical scheme,

$$u^{n+1} = \mathrm{e}^{\Theta_m(t_{n+1},t_n)}u^n, \tag{2.2}$$

where $t_n = t_0 + nh$, h is the time step, u^n is an approximation to the exact solution at t_n, and $\Theta_m(t,s)$ is a finite truncation of the Magnus expansion $\Theta(t,s)$ whose exponential evolves the exact solution from s to t.

As mentioned in the introduction, for the sake of simplicity, we will restrict ourselves to the one dimensional case in subsections 2.1–2.4. The results are extended to higher dimensions in subsection 2.5.

2.1 Simplified-commutator Magnus expansions

In the semiclassical regime, the order two and order four simplified-commutator Magnus expansions of (Iserles et al. 2018) that preserve the integral become

$$\begin{aligned}\Theta_0(h) &= \mathrm{i}h\varepsilon\partial_x^2 - \mathrm{i}\varepsilon^{-1}\mu_{0,0}(h),\\ \Theta_2(h) &= \mathrm{i}h\varepsilon\partial_x^2 - \mathrm{i}\varepsilon^{-1}\mu_{0,0}(h) - 2\left\langle\partial_x\mu_{1,1}(h)\right\rangle_1,\end{aligned}$$

respectively. This follows directly from the results of (Iserles et al. 2018) by accounting for the additional scalar factors ε and ε^{-1}. The quantities $\mu_{0,0}(h)$ and $\mu_{1,1}(h)$ have been already introduced earlier and

$$\langle f\rangle_k := \tfrac{1}{2}\left(f\circ\partial_x^k + \partial_x^k\circ f\right), \quad k\geq 0,\ f\in \mathrm{C}_p^\infty(I;\mathbb{R}) \tag{2.3}$$

are the symmetrised differential operators which first appeared in (Bader et al. 2014), and have been studied in detail in (Singh 2015, Singh 2017). These operators are used here for the same reasons as in (Bader et al. 2014, Bader et al. 2016, Iserles et al. 2018) – namely, for preservation of unitarity under discretisation after simplification of commutators and, consequently, stability of the method.

2.2 Analysis of size

As a consequence of (1.3), the symmetrised differential operators scale as

$$\langle f\rangle_k \rightsquigarrow \tfrac{1}{2}\left(\mathcal{D}_f\mathcal{K}_k + \mathcal{K}_k\mathcal{D}_f\right) = \mathcal{O}\left(\varepsilon^{-k}\right) \tag{2.4}$$

upon discretisation, assuming that f is independent of ε. For convenience, we abuse notation[4] somewhat and use the shorthand $\langle f\rangle_k = \mathcal{O}\left(\varepsilon^{-k}\right)$ instead of (2.4).

Theorem 1 *All nested commutators of $\varepsilon\partial_x^2$, $\varepsilon^{-1}V$ and, in general, terms of the form $\varepsilon^k \langle f\rangle_{k+1}$ are $\mathcal{O}\left(\varepsilon^{-1}\right)$ or smaller (Singh 2015, Singh 2017).*

Thus a grade p (i.e. $p-1$ times nested) commutator of $\mathrm{i}h\varepsilon\partial_x^2$ and $-\mathrm{i}h\varepsilon^{-1}V$, which is typically considered to be $\mathcal{O}\left(h^p\right)$, without accounting for ε or growth corresponding to finer spatial discretisation, becomes $\mathcal{O}\left(h^p\varepsilon^{-1}\right)$ when analysed taking all factors into account.

To unify the analysis of magnitude of terms, we express the time step in terms of the inherent parameter ε,

$$h = \mathcal{O}\left(\varepsilon^{\sigma}\right), \quad \sigma > 0, \tag{2.5}$$

where a smaller σ corresponds to larger time steps. We will be aiming to develop methods that work for small values of σ and at the very least we may assume that $\sigma \leq 1$.

Taylor expansion for an analytic potential, $V(\xi) = \sum_{k=0}^{\infty}[V^{(k)}(0)/k!]\xi^k$, shows that $\mu_{1,1}(h) = \int_0^h (\xi - h/2)V(\xi)d\xi$ is $\mathcal{O}\left(h^3\right)$ for smooth potentials, since its $\mathcal{O}\left(h^2\right)$ term, $V^{(0)}(0)\int_0^h(\xi-h/2)d\xi$, vanishes.

Combining all these ingredients, we conclude that

$$\Theta_2(h) = \overbrace{\mathrm{i}h\varepsilon\partial_x^2}^{\mathcal{O}\left(\varepsilon^{\sigma-1}\right)} - \overbrace{\mathrm{i}\varepsilon^{-1}\mu_{0,0}(h)}^{\mathcal{O}\left(\varepsilon^{\sigma-1}\right)} - \overbrace{2\left\langle\partial_x\mu_{1,1}(h)\right\rangle_1}^{\mathcal{O}\left(\varepsilon^{3\sigma-1}\right)}. \tag{2.6}$$

Here it becomes evident that the two leading terms in the Magnus expansion are significantly larger than the trailing terms. As mentioned in the introduction, the direct usage of Lanczos iterations for $\exp(\Theta_2)$ is costly due to the $\mathcal{O}\left(\varepsilon^{\sigma-1}\right)$ growth of the leading terms.

On the other hand, the large term $\mathrm{i}h\varepsilon\partial_x^2$ can be exponentiated via FFTs at a $\mathcal{O}\left(N\log N\right)$ cost since it discretises as a circulant matrix and the diagonal term

[4] This notion can be made more rigorous by noting that in the semiclassical regime the derivatives of the solution grow as $\left\|\partial_x^k u\right\|_2 \leq C_k\varepsilon^{-k}$, and consequently $\left\|\langle f\rangle_k(u)\right\|_2 \leq C_k\|f\|\varepsilon^{-k}$. The analysis of the methods presented here can be made rigorous in accordance with these observations. See (Singh 2015, Singh 2017) for details.

$\mathrm{i}\varepsilon^{-1}\mu_{0,0}(h)$ can be exponentiated directly at the cost of $\mathcal{O}(N)$ operations. Thus, we resort to Zassenhaus splittings to separate these vastly disparate scales, whereby only the small $\mathcal{O}\left(\varepsilon^{3\sigma-1}\right)$ terms need be exponentiated via Lanczos iterations. The small size of the remaining exponents means we can work with large time steps (a small σ, say $\sigma = 1/2$ for instance) and still require very few Lanczos iterations.

2.3 Symmetric Zassenhaus splitting

In order to split the exponential of the fourth-order Magnus expansion, Θ_2, using Zassenhaus splitting algorithm, we follow the procedure outlined in Appendix B. In particular, the exponential we wish to approximate here is e^{Θ_2}. Thus, we take $\mathcal{W}^{[0]} = \Theta_2$, which needs to be split in two components, $X = W^{[0]}$ and $Y = \mathcal{W}^{[0]} - W^{[0]}$. We usually prefer to extract the largest terms first yet we may choose between $W^{[0]} = \mathrm{i}h\varepsilon\partial_x^2$ and $W^{[0]} = -\mathrm{i}\varepsilon^{-1}\mu_{0,0}(h)$, which are both $\mathcal{O}\left(h\varepsilon^{-1}\right) = \mathcal{O}\left(\varepsilon^{\sigma-1}\right)$.

In the specific method presented here, we opt for the former, whereby $X = W^{[0]} = \mathrm{i}h\varepsilon\partial_x^2 = \mathrm{i}h\varepsilon\left\langle 1\right\rangle_2$ and $Y = \mathcal{W}^{[0]} - W^{[0]} = -\mathrm{i}\varepsilon^{-1}\left\langle\mu_{0,0}(h)\right\rangle_0 - 2\left\langle\partial_x\mu_{1,1}(h)\right\rangle_1$. (Observe that $\left\langle 1\right\rangle_k = \partial_x^k$ and $\left\langle f\right\rangle_0 = f$. We will switch between these equivalent notations at our convenience.) Using the sBCH formula (B.1), we write

$$\mathrm{e}^{\Theta_2} = \mathrm{e}^{\mathcal{W}^{[0]}} = \mathrm{e}^{\frac{1}{2}\mathrm{i}h\varepsilon\partial_x^2}\mathrm{e}^{\mathcal{W}^{[1]}}\mathrm{e}^{\frac{1}{2}\mathrm{i}\varepsilon h\partial_x^2} + \mathcal{O}\left(h^5\varepsilon^{-1}\right), \tag{2.7}$$

where, using the order four expression for $\mathcal{W}^{[1]} = \mathrm{sBCH}(-X, X+Y)$ from (B.4),

$$\begin{aligned}\mathcal{W}^{[1]} = &-\mathrm{i}\varepsilon^{-1}\left\langle\mu_{0,0}(h)\right\rangle_0 - 2\left\langle\partial_x\mu_{1,1}(h)\right\rangle_1 + \tfrac{1}{24}\mathrm{i}h^2\varepsilon[[\left\langle\mu_{0,0}(h)\right\rangle_0, \left\langle 1\right\rangle_2], \left\langle 1\right\rangle_2] \\ &+\tfrac{1}{12}h^2\varepsilon^2[[\left\langle\partial_x\mu_{1,1}(h)\right\rangle_1, \left\langle 1\right\rangle_2], \left\langle 1\right\rangle_2] - \tfrac{1}{12}\mathrm{i}h\varepsilon^{-1}[[\left\langle\mu_{0,0}(h)\right\rangle_0, \left\langle 1\right\rangle_2], \left\langle\mu_{0,0}(h)\right\rangle_0] \\ &-\tfrac{1}{6}h[[\left\langle\mu_{0,0}(h)\right\rangle_0, \left\langle 1\right\rangle_2], \left\langle\partial_x\mu_{1,1}(h)\right\rangle_1] - \tfrac{1}{6}h[[\left\langle\partial_x\mu_{1,1}(h)\right\rangle_1, \left\langle 1\right\rangle_2], \left\langle\mu_{0,0}(h)\right\rangle_0] \\ &+\tfrac{1}{3}\mathrm{i}h\varepsilon[[\left\langle\partial_x\mu_{1,1}(h)\right\rangle_1, \left\langle 1\right\rangle_2], \left\langle\partial_x\mu_{1,1}(h)\right\rangle_1] + \mathcal{O}\left(h^5\varepsilon^{-1}\right),\end{aligned} \tag{2.8}$$

and we have ignored all $\mathcal{O}\left(h^5\varepsilon^{-1}\right) = \mathcal{O}\left(\varepsilon^{5\sigma-1}\right)$ terms in the sBCH since this is also the error inherent in our Magnus expansion.

Further, we observe that

$$\begin{aligned}\mathcal{W}^{[1]} = &-\mathrm{i}\varepsilon^{-1}\left\langle\mu_{0,0}(h)\right\rangle_0 - 2\left\langle\partial_x\mu_{1,1}(h)\right\rangle_1 + \tfrac{1}{24}\mathrm{i}h^2\varepsilon[[\left\langle\mu_{0,0}(h)\right\rangle_0, \left\langle 1\right\rangle_2], \left\langle 1\right\rangle_2] \\ &-\tfrac{1}{12}\mathrm{i}h\varepsilon^{-1}[[\left\langle\mu_{0,0}(h)\right\rangle_0, \left\langle 1\right\rangle_2], \left\langle\mu_{0,0}(h)\right\rangle_0] + \mathcal{O}\left(h^5\varepsilon^{-1}\right),\end{aligned} \tag{2.9}$$

since most commutators are $\mathcal{O}\left(h^5\varepsilon^{-1}\right)$ or smaller due to Theorem 1 and the observation that $\mu_{0,0}(h) = \mathcal{O}(h)$ and $\mu_{1,1}(h) = \mathcal{O}\left(h^3\right)$. These nested commutators can be simplified using the identities (A.1), the detailed theory for which is presented in (Singh 2015) and which were utilised in the derivation of the simplified-commutator Magnus expansion Θ_2 in (Iserles et al. 2018). Applying these identities, we find

$$\begin{aligned}[\left\langle\mu_{0,0}(h)\right\rangle_0, \left\langle 1\right\rangle_2] &= -2\left\langle\partial_x\mu_{0,0}(h)\right\rangle_1, \\ \left[[\left\langle\mu_{0,0}(h)\right\rangle_0, \left\langle 1\right\rangle_2], \left\langle 1\right\rangle_2\right] &= 4\left\langle\partial_x^2\mu_{0,0}(h)\right\rangle_2 - \left\langle\partial_x^4\mu_{0,0}(h)\right\rangle_0, \\ \left[\left\langle\partial_x\mu_{1,1}(h)\right\rangle_1, \left\langle 1\right\rangle_2\right] &= -2\left\langle\partial_x^2\mu_{1,1}(h)\right\rangle_2 + \tfrac{1}{2}\left\langle\partial_x^4\mu_{1,1}(h)\right\rangle_0, \\ \left[[\left\langle\mu_{0,0}(h)\right\rangle_0, \left\langle 1\right\rangle_2], \left\langle\mu_{0,0}(h)\right\rangle_0\right] &= -2\left\langle(\partial_x\mu_{0,0}(h))^2\right\rangle_0.\end{aligned} \tag{2.10}$$

Thus, the central exponent in (2.7) up to $\mathcal{O}\left(h^5\varepsilon^{-1}\right) = \mathcal{O}\left(\varepsilon^{5\sigma-1}\right)$ is

$$\begin{aligned}\mathcal{W}^{[1]} = &-\mathrm{i}\varepsilon^{-1}\left\langle\mu_{0,0}(h)\right\rangle_0 + \tfrac{1}{6}\mathrm{i}h^2\varepsilon\left\langle\partial_x^2\mu_{0,0}(h)\right\rangle_2 - 2\left\langle\partial_x\mu_{1,1}(h)\right\rangle_1 \\ &-\tfrac{1}{24}\mathrm{i}h^2\varepsilon\left\langle\partial_x^4\mu_{0,0}(h)\right\rangle_0 + \tfrac{1}{6}\mathrm{i}h\varepsilon^{-1}\left\langle\left(\partial_x\mu_{0,0}(h)\right)^2\right\rangle_0.\end{aligned} \tag{2.11}$$

In order to approximate the exponential of $\mathcal{W}^{[1]}$ (which is required in (2.7)), we apply the sBCH again along the lines of (2.7), writing

$$\mathrm{e}^{\mathcal{W}^{[1]}} = \mathrm{e}^{-\frac{1}{2}\mathrm{i}\varepsilon^{-1}\mu_{0,0}(h)}\mathrm{e}^{\mathcal{W}^{[2]}}\mathrm{e}^{-\frac{1}{2}\mathrm{i}\varepsilon^{-1}\mu_{0,0}(h)} + \mathcal{O}\left(h^5\varepsilon^{-1}\right). \tag{2.12}$$

Here we have chosen to extract the largest term $X = W^{[1]} = -\mathrm{i}\varepsilon^{-1}\mu_{0,0}(h) = \mathcal{O}\left(h\varepsilon^{-1}\right)$ and the remainder is $Y = \mathcal{W}^{[1]} - W^{[1]} = \mathcal{O}\left(h^3\varepsilon^{-1}\right)$. The choice of X is more obvious in this case since there is only one term of size $\mathcal{O}\left(h\varepsilon^{-1}\right)$. Keeping the sizes of X and Y in mind, we find that

$$\begin{aligned}\mathcal{W}^{[2]} &:= \mathrm{sBCH}(-X, X+Y) + \mathcal{O}\left(h^5\varepsilon^{-1}\right) = \left(-X + (X+Y)\right) = Y + \mathcal{O}\left(h^5\varepsilon^{-1}\right) \\ &= \tfrac{1}{6}\mathrm{i}h^2\varepsilon\left\langle\partial_x^2\mu_{0,0}(h)\right\rangle_2 - 2\left\langle\partial_x\mu_{1,1}(h)\right\rangle_1 \\ &\quad - \tfrac{1}{24}\mathrm{i}h^2\varepsilon\left\langle\partial_x^4\mu_{0,0}(h)\right\rangle_0 + \tfrac{1}{6}\mathrm{i}h\varepsilon^{-1}\left\langle\left(\partial_x\mu_{0,0}(h)\right)^2\right\rangle_0 + \mathcal{O}\left(h^5\varepsilon^{-1}\right)\end{aligned} \tag{2.13}$$

suffices up to $\mathcal{O}\left(h^5\varepsilon^{-1}\right)$ since $[[Y,X],X]$ and $[[Y,X],Y]$ are $\mathcal{O}\left(h^5\varepsilon^{-1}\right)$ and $\mathcal{O}\left(h^7\varepsilon^{-1}\right)$, respectively. Further, we discard the $\mathcal{O}\left(h^3\varepsilon\right)$ term $-\frac{1}{24}\mathrm{i}h^2\varepsilon\left\langle\partial_x^4\mu_{0,0}(h)\right\rangle_0$ from (2.13) since, under the assumption $\sigma \le 1$, it is effectively $\mathcal{O}\left(\varepsilon^{5\sigma-1}\right)$ or smaller.

Finally, we complete the derivation of our fourth-order based Magnus–Zassenhaus splitting by combining (2.7) and (2.12),

$$\exp(\Theta_2) = \mathrm{e}^{\frac{1}{2}W^{[0]}}\mathrm{e}^{\frac{1}{2}W^{[1]}}\mathrm{e}^{\mathcal{W}^{[2]}}\mathrm{e}^{\frac{1}{2}W^{[1]}}\mathrm{e}^{\frac{1}{2}W^{[0]}} + \mathcal{O}\left(\varepsilon^{5\sigma-1}\right), \tag{2.14}$$

which has the same form as the splittings described in Appendix B. Here the exponents (chosen and/or computed during the derivation) are

$$\begin{aligned}&W^{[0]} = \mathrm{i}h\varepsilon\partial_x^2 = \mathcal{O}\left(\varepsilon^{\sigma-1}\right), \\ &W^{[1]} = -\mathrm{i}\varepsilon^{-1}\mu_{0,0}(h) = \mathcal{O}\left(\varepsilon^{\sigma-1}\right), \\ &\mathcal{W}^{[2]} = \tfrac{1}{6}\mathrm{i}h\varepsilon^{-1}\left(\partial_x\mu_{0,0}(h)\right)^2 - 2\left\langle\partial_x\mu_{1,1}(h)\right\rangle_1 + \tfrac{1}{6}\mathrm{i}h^2\varepsilon\left\langle\partial_x^2\mu_{0,0}(h)\right\rangle_2 = \mathcal{O}\left(\varepsilon^{3\sigma-1}\right).\end{aligned} \tag{2.15}$$

Since the total number of time steps required to reach a final time T grows as $T/h = \mathcal{O}\left(\varepsilon^{-\sigma}\right)$, the global accuracy of this method is $\mathcal{O}\left(\varepsilon^{4\sigma-1}\right)$.

It is only by this stage – having arrived at an asymptotic splitting expressed in operatorial terms – that we start considering discretisation issues. Apart from analysis of size, considerations of spatial and temporal discretisation (in the form of approximation through quadrature) are entirely independent of the procedure leading to (2.15) and of each other: one may proceed to address them in any order.

Remark 2 *Note that, in contrast to the Magnus–Zassenhaus splitting of (Bader et al. 2016), our exponents retain the integrals intact (in $\mu_{0,0}(h)$ and $\mu_{1,1}(h)$). This provides us with the flexibility to choose the most suitable approximation method including the possibility of analytic approximations. This flexibility proves particularly helpful in the case of potentials with high temporal oscillations.*

Remark 3 *As a quick sanity check, we do arrive at the standard symmetric Zassenhaus splitting (Bader et al. 2014) for time-independent potentials, $V(x,t) := V(x)$.*

Remark 4 *Discarding terms such as the $\mathcal{O}\left(h^3\varepsilon\right)$ term $-\frac{1}{24}\mathrm{i}h^2\varepsilon\left\langle\partial_x^4\mu_{0,0}(h)\right\rangle_0$ means that (2.14) is not a fourth-order scheme in terms of h. In principle such terms can be retained in order to derive schemes that are both, fourth-order in h and order $4\sigma-1$ in ε. Such schemes may feature a lower error constant at the expense of more terms (particularly when ε is only moderately small). The number of the additional terms (and derivatives of the potential) to be retained may grow rapidly with the order, however. Since our primary aim is to seek methods that allow use of relatively large time steps in presence of small ε, the development of high-order methods in h is not pursued in this manuscript.*

2.4 Implementation

The operatorial splitting given by (2.14) and (2.15) can be converted into a concrete numerical scheme by resorting to spatial discretisation. As typical, we use spectral collocation, whereby $W^{[0]}$ is discretised as the circulant matrix[5] $\widetilde{W^{[0]}} = \mathrm{i}h\varepsilon\mathcal{K}_2$. Note that $\mathcal{K}_2$ is diagonalisable via Fourier transform since

$$\mathcal{K}_k = \mathcal{F}^{-1}\mathcal{D}_{c_k}\mathcal{F}, \tag{2.16}$$

where c_k is the symbol of $\mathcal{K}_k$, $\mathcal{F}$ is the Fast Fourier Transform (FFT) and $\mathcal{F}^{-1}$ is its inverse (IFFT). Thus, we can evaluate

$$\mathrm{e}^{\frac{1}{2}\widetilde{W^{[0]}}}\boldsymbol{u} = \mathcal{F}^{-1}\mathcal{D}_{\exp(\frac{1}{2}\mathrm{i}h\varepsilon c_2)}\mathcal{F}\boldsymbol{u},$$

in $\mathcal{O}\left(N\log N\right)$ operations. The next exponent, $W^{[1]}$, is discretised as the diagonal matrix $\widetilde{W^{[1]}} = -\mathrm{i}\varepsilon^{-1}\mathcal{D}_{\mu_{0,0}(h)}$ and exponentiated pointwise in $\mathcal{O}\left(N\right)$ operations,

$$\mathrm{e}^{\frac{1}{2}\widetilde{W^{[1]}}}\boldsymbol{u} = \mathcal{D}_{\exp(\frac{1}{2}\mathrm{i}\varepsilon^{-1}\mu_{0,0}(h))}\boldsymbol{u}.$$

Lastly, the innermost exponent,

$$\begin{aligned}\mathcal{W}^{[2]} \rightsquigarrow \widetilde{\mathcal{W}^{[2]}} = {}& \tfrac{1}{6}\mathrm{i}h\varepsilon^{-1}\mathcal{D}_{(\partial_x\mu_{0,0}(h))^2} + \left(\mathcal{K}_1\mathcal{D}_{\partial_x\mu_{1,1}(h)} + \mathcal{D}_{\partial_x\mu_{1,1}(h)}\mathcal{K}_1\right)\\ & -\tfrac{1}{3}\mathrm{i}h^2\varepsilon\left(\mathcal{K}_2\mathcal{D}_{\partial_x^2\mu_{0,0}(h)} + \mathcal{D}_{\partial_x^2\mu_{0,0}(h)}\mathcal{K}_2\right),\end{aligned}$$

which is neither circulant nor diagonal, can be very effectively exponentiated via Lanczos iterations because (unlike the first two exponents) it is very small in size, even when combined with large time steps.

For instance, when using time steps as large as $h = \mathcal{O}\left(\varepsilon^{1/2}\right)$, i.e. under the scaling $\sigma = 1/2$, the exponent $\widetilde{\mathcal{W}^{[2]}}$ is $\mathcal{O}\left(\varepsilon^{1/2}\right)$. As the semiclassical parameter $\varepsilon \ll 1$ becomes small, this spectral radius approaches 0. Thus the superlinear accuracy of Lanczos iterations is seen immediately and merely three Lanczos iterations are required for an exponentiation to an accuracy of $\mathcal{O}\left(\varepsilon^{5\sigma-1}\right) = \mathcal{O}\left(\varepsilon^{3/2}\right)$, which is the accuracy of the

[5] In the one-dimensional case we drop the first index, writing $\mathcal{K}_k$ instead of $\mathcal{K}_{1,k}$.

splitting. A more detailed analysis of the number of Lanczos iterations required for such exponents is carried out in (Bader et al. 2014, Bader et al. 2016).

Each Lanczos iteration requires the computation of a matrix–vector product of the form $\widetilde{\mathcal{W}^{[2]}}\boldsymbol{v}$. In general Lanczos iterations for the discretisation of $W = \sum_{k=0}^{n} \mathrm{i}^{k+1} \langle f_k \rangle_k$ to $\widetilde{W} = \mathrm{i}\mathcal{D}_{f_0} + \frac{1}{2}\sum_{k=1}^{n} \mathrm{i}^{k+1} (\mathcal{D}_{f_k}\mathcal{K}_k + \mathcal{K}_k\mathcal{D}_{f_k})$ can be efficiently computed in $2n+2$ Fast Fourier Transforms (included inverses) using the expression

$$\widetilde{W}\boldsymbol{v} = \mathrm{i}\mathcal{D}_{f_0}\boldsymbol{v} + \tfrac{1}{2}\left(\sum_{k=1}^{n} \mathrm{i}^{k+1}\mathcal{D}_{f_k}\mathcal{F}^{-1}\mathcal{D}_{c_k}\right)\mathcal{F}\boldsymbol{v} + \tfrac{1}{2}\mathcal{F}^{-1}\left(\sum_{k=1}^{n} \mathrm{i}^{k+1}\mathcal{D}_{c_k}\mathcal{F}\mathcal{D}_{f_k}\boldsymbol{v}\right) \quad (2.17)$$

Thus, the computation of $\widetilde{\mathcal{W}^{[2]}}\boldsymbol{v}$ in each Lanczos iteration requires six FFTs and the total cost of its exponentiation is 18 FFTs. This completes the derivation of the splitting described in (1.5).

Remark 5 *Θ_0 is an order two Magnus expansion. An order two Zassenhaus splitting is merely the Strang splitting. Thus an order two Magnus–Zassenhaus splitting is, trivially, (1.4), which has been presented in the introduction. Note that (1.4) happens to be order two in h and order $2\sigma - 1$ in ε, simultaneously.*

Remark 6 *We assume that the integrals $\mu_{0,0}(h)$ and $\mu_{1,1}(h)$ are either available analytically or can be adequately approximated via quadrature formulae such as Gauss–Legendre quadratures, along the lines of (Iserles et al. 2018).*

Remark 7 *Along the lines of (Bader et al. 2016, Iserles et al. 2018), we also assume that spatial derivatives of the potential, as well as its integrals, are either available or inexpensive to compute.*

2.5 Extension to higher dimensions

The fourth-order Magnus expansion (2.3) is easily extended to the d-dimensional case,

$$\Theta_2(h) = \mathrm{i}h\varepsilon\Delta - \mathrm{i}\varepsilon^{-1}\mu_{0,0}(h) - 2\sum_{j=1}^{d} \langle \partial_j \mu_{1,1}(h) \rangle_{(j,1)}\,, \quad (2.18)$$

using $[\Delta, f] = \sum_{j=1}^{d} [\partial_j^2, f] = 2\sum_{j=1}^{d} \langle \partial_j f \rangle_{(j,1)}$, where we define

$$\langle f \rangle_{(j,k)} = \tfrac{1}{2}\left(f \circ \partial_j^k + \partial_j^k \circ f\right).$$

A symmetric Zassenhaus splitting for this Magnus expansion proceeds along the same lines as the procedure carried out for the one-dimensional case in subsection 2.3. Extracting $W^{[0]} = \mathrm{i}h\varepsilon\Delta$ and $W^{[1]} = -\mathrm{i}\varepsilon^{-1}\mu_{0,0}(h)$ in the first two steps, the central exponent in the Zassenhaus splitting is

$$\begin{aligned}\mathcal{W}^{[2]} = {} & -2\sum_{j=1}^{d} \langle \partial_j \mu_{1,1}(h) \rangle_{(j,1)} + \tfrac{1}{24}\mathrm{i}h^2\varepsilon[[\mu_{0,0}(h), \Delta], \Delta] \\ & -\tfrac{1}{12}\mathrm{i}h\varepsilon^{-1}[[\mu_{0,0}(h), \Delta], \mu_{0,0}(h)] + \mathcal{O}\left(h^5\varepsilon^{-1}\right). \end{aligned} \quad (2.19)$$

What remains in the derivation is the simplification of nested commutators along the lines of (2.10) which have a d-dimensional generalisations that can be verified by using the chain rule,

$$[[\mu_{0,0}(h),\Delta],\mu_{0,0}(h)] = \sum_{j=1}^{d}[[\mu_{0,0}(h),\partial_j^2],\mu_{0,0}(h)] = -2\sum_{j=1}^{d}(\partial_j\mu_{0,0}(h))^2$$
$$[[\mu_{0,0}(h),\Delta],\Delta] = 4\sum_{i,j=1}^{d}\langle\partial_i\partial_j\mu_{0,0}(h)\rangle_{(i,1),(j,1)} - \sum_{i,j=1}^{d}(\partial_i^2\partial_j^2\mu_{0,0}(h)),$$

where $\langle f\rangle_{(i,l),(j,k)} = \frac{1}{2}\left(f\circ\partial_i^l\partial_j^k + \partial_i^l\partial_j^k\circ f\right)$.

Consequently, the exponents in the Zassenhaus splitting (2.14) in d-dimensions, under the scaling $h=\mathcal{O}\left(\varepsilon^{\sigma}\right),\sigma\le 1$, are $W^{[0]}=\mathrm{i}h\varepsilon\Delta$, $W^{[1]}=-\mathrm{i}\varepsilon^{-1}\mu_{0,0}(h)$ and

$$\mathcal{W}^{[2]} = \sum_{j=1}^{d}\left[\tfrac{1}{6}\mathrm{i}h\varepsilon^{-1}(\partial_j\mu_{0,0}(h))^2 - 2\left\langle\partial_j\mu_{1,1}(h)\right\rangle_{(j,1)} + \tfrac{1}{6}\mathrm{i}h^2\varepsilon\left\langle\partial_j^2\mu_{0,0}(h)\right\rangle_{(j,2)}\right]$$
$$+\tfrac{1}{3}\mathrm{i}h^2\varepsilon\sum_{i=1}^{d-1}\sum_{j=i+1}^{d}\langle\partial_i\partial_j\mu_{0,0}(h)\rangle_{(i,1),(j,1)} + \mathcal{O}\left(\varepsilon^{5\sigma-1}\right).$$

Here the expression $-\frac{1}{24}\mathrm{i}h^2\varepsilon\sum_{i,j=1}^{d}(\partial_i^2\partial_j^2\mu_{0,0}(h))$ is $\mathcal{O}\left(\varepsilon^{5\sigma-1}\right)$ or smaller and has been discarded from $\mathcal{W}^{[2]}$, as before.

Thus, the extension to d dimensions involves a dimension-wise sum of terms appearing in the central exponent of (2.15) plus an additional term where mixed derivatives appear. In particular, in the case of three dimensions, this involves three mixed derivatives $\partial_x\partial_y,\partial_x\partial_z$ and $\partial_y\partial_z$.

3 Sixth-order based Magnus–Zassenhaus splitting

The sixth-order based simplified-commutator Magnus expansion of (Iserles et al. 2018) in the context of the semiclassical regime, is

$$\Theta_4(h) = \overbrace{\mathrm{i}h\varepsilon\partial_x^2 - \mathrm{i}\varepsilon^{-1}\mu_{0,0}(h)}^{\mathcal{O}\left(h\varepsilon^{-1}\right)} - \overbrace{2\left\langle\partial_x\mu_{1,1}(h)\right\rangle_1}^{\mathcal{O}\left(h^3\varepsilon^{-1}\right)} + \overbrace{\mathrm{i}\varepsilon^{-1}\Lambda\left[\psi\right]_{1,1}(h) + 2\mathrm{i}\varepsilon\left\langle\partial_x^2\mu_{2,1}(h)\right\rangle_2}^{\mathcal{O}\left(h^4\varepsilon^{-1}\right)}$$
$$+\overbrace{\tfrac{1}{6}\left\langle\Lambda\left[\varphi_1\right]_{1,2}(h)+\Lambda\left[\varphi_2\right]_{2,1}(h)\right\rangle_1}^{\mathcal{O}\left(h^4\varepsilon^{-1}\right)} + \overbrace{\tfrac{1}{6}\left\langle\Lambda\left[\phi_1\right]_{1,2}(h)+\Lambda\left[\phi_2\right]_{2,1}(h)\right\rangle_1}^{\mathcal{O}\left(h^5\varepsilon^{-1}\right)}$$
$$+\overbrace{\tfrac{4}{3}\varepsilon^2\left\langle\partial_x^3\mu_{3,1}(h)\right\rangle_3}^{\mathcal{O}\left(h^5\varepsilon^{-1}\right)} + \overbrace{\tfrac{1}{4}\mathrm{i}\varepsilon\partial_x^4\mu_{2,1}(h)}^{\mathcal{O}\left(h^4\varepsilon\right)} = \Theta(h) + \mathcal{O}\left(\varepsilon^{7\sigma-1}\right), \tag{3.1}$$

where $\mu_{j,k}(h)$ are integrals on the line,

$$\mu_{j,k}(h) = \int_0^h \tilde{B}_j^k(h,\zeta)V(\zeta)\,\mathrm{d}\zeta, \tag{3.2}$$

$\Lambda[f]_{a,b}(h)$ are integrals over a triangle,

$$\Lambda[f]_{a,b}(h) = \int_0^h \int_0^\zeta f(h,\zeta,\xi)\left[\partial_x^a V(\zeta)\right]\left[\partial_x^b V(\xi)\right]\,\mathrm{d}\xi\,\mathrm{d}\zeta, \tag{3.3}$$

$\tilde{B}_j(h,\zeta) = h^j B_j(\zeta/h)$ are rescaled Bernoulli polynomials (Abramowitz & Stegun 1964, Lehmer 1988), and

$$\begin{aligned}
\psi(h,\zeta,\xi) &= \zeta - \xi - \tfrac{h}{3},\\
\varphi_1(h,\zeta,\xi) &= h^2 - 4h\xi + 2\zeta\xi,\\
\varphi_2(h,\zeta,\xi) &= (h-2\zeta)^2 - 2\zeta\xi,\\
\phi_1(h,\zeta,\xi) &= h^2 - 6h\zeta + 6h\xi + 6\zeta\xi + 3\zeta^2 - 12\xi^2,\\
\phi_2(h,\zeta,\xi) &= h^2 - 6h\zeta + 6h\xi - 6\zeta\xi + 5\zeta^2.
\end{aligned}$$

Remark 8 *Note that, since* $B_0(x) = 1$,

$$\mu_{0,k}(h) = \mu_{j,0}(h) = \mu_{0,0}(h), \quad j,k \in \mathbb{Z}^+.$$

To avoid confusion, therefore, such terms will always be indexed as $\mu_{0,0}(h)$.

3.1 Size analysis

Size of the terms is analysed with the aid of Lemmas 2 and 3.

Lemma 2 *For an analytic potential* V,

$$\mu_{j,k}(h) = \mathcal{O}\left(h^{jk+1}\right), \quad k \neq 1, \qquad \mu_{j,1}(h) = \mathcal{O}\left(h^{j+2}\right). \tag{3.4}$$

Proof *Since the* jth *rescaled Bernoulli polynomial scales as* $\mathcal{O}\left(h^j\right)$, *we expect* $\mu_{j,k}(h) = \mathcal{O}\left(h^{jk+1}\right)$. *The term* $\mu_{j,1}(h)$ *gains an extra power of* h *and is* $\mathcal{O}\left(h^{j+2}\right)$ *since integrals of Bernoulli polynomials vanish,* $\int_0^h \tilde{B}_j(h,\zeta)\,\mathrm{d}\zeta = 0$. *To see this, consider the Taylor expansion,* $V(\zeta) = \sum_{n=0}^\infty [V^{(n)}/n!]\zeta^n$, *and note that in the expansion for* $\mu_{j,1}(h)$, *the leading order term* $\int_0^h V^{(0)}\tilde{B}_j(h,\zeta)\,\mathrm{d}\zeta = 0$ *vanishes.*

□

Lemma 3 *In general, for a polynomial* $r_n(h,\zeta,\xi)$ *featuring only degree-*n *terms in* h,ζ *and* ξ, *the linear (integral) functional is*

$$\Lambda[r_n]_{a,b}(h) = \mathcal{O}\left(h^{n+2}\right). \tag{3.5}$$

For a polynomial p_n *whose integral over the triangle vanishes,* $\int_0^h\int_0^\zeta p_n(h,\zeta,\xi)\,\mathrm{d}\xi\,\mathrm{d}\zeta = 0$, *we gain an extra power of* h *and*

$$\Lambda[p_n]_{a,b}(h) = \mathcal{O}\left(h^{n+3}\right). \tag{3.6}$$

In particular, this happens for ψ, ϕ_1 *and* ϕ_2, *but not for* φ_1 *and* φ_2.

3.2 Reduction of stages in Zassenhaus splitting

The expansion (3.1) features both odd and even powers of h – in particular, it features terms of size $\mathcal{O}\left(h^4\varepsilon^{-1}\right)$. When we commence the Zassenhaus procedure directly from Θ_4, the resulting exponential splitting

$$\mathrm{e}^{\frac{1}{2}W^{[0]}}\mathrm{e}^{\frac{1}{2}W^{[1]}}\mathrm{e}^{\frac{1}{2}W^{[2]}}\mathrm{e}^{\frac{1}{2}W^{[3]}}\mathrm{e}^{\frac{1}{2}W^{[4]}}\mathrm{e}^{\mathcal{W}^{[5]}}\mathrm{e}^{\frac{1}{2}W^{[4]}}\mathrm{e}^{\frac{1}{2}W^{[3]}}\mathrm{e}^{\frac{1}{2}W^{[2]}}\mathrm{e}^{\frac{1}{2}W^{[1]}}\mathrm{e}^{\frac{1}{2}W^{[0]}}, \tag{3.7}$$

features exponents $W^{[3]} = \mathcal{O}\left(h^4\varepsilon^{-1}\right)$ and $\mathcal{W}^{[5]} = \mathcal{O}\left(h^6\varepsilon^{-1}\right)$ and the power of h is even. Similarly, symmetric Zassenhaus splitting of a higher order Magnus expansion such as Θ_8 also features $\mathcal{O}\left(h^4\varepsilon^{-1}\right)$, $\mathcal{O}\left(h^6\varepsilon^{-1}\right)$, $\mathcal{O}\left(h^8\varepsilon^{-1}\right)$ and $\mathcal{O}\left(h^{10}\varepsilon^{-1}\right)$ exponents.

In contrast, the Zassenhaus splittings of (Bader et al. 2014) and (Bader et al. 2016), only feature exponents in odd powers of h: even powers of h do not appear in (Bader et al. 2016) since the integrals in the Magnus expansion are discretised at the outset by Gaussian quadrature. The appearance of even powers of h is suboptimal because it results in a larger number of exponentials here.

To remedy this, we note that the results of (Iserles et al. 2018), from which we have commenced our analysis, are based on power truncated Magnus expansions. These methods are known to be odd in h around the midpoint of the interval ($t_{1/2} = t + h/2$) due to time symmetry of the flow (Iserles et al. 2000, Iserles, Nørsett & Rasmussen 2001).

It should, therefore, be possible to expand Θ_m solely in odd powers of h for any choice of the potential V. A Zassenhaus splitting commencing from such an odd-powered expansion will never introduce even powers of h since underlying the procedure is a recursive application of the symmetric BCH which features only odd-grade commutators. Consequently, in contrast to the eleven exponentials appearing in (3.7), the Magnus–Zassenhaus splitting (3.18) that we are about to develop later in this section features just seven exponentials.

Remark 9 *The extra stages appearing in (3.7) can also be seen as a consequence of lack of symmetry of the scheme.*

3.3 Time symmetry and shifting the origin

In this section we derive an expression for Θ_4 expanded solely in odd powers of h. Recall that, in order to advance from time t to $t + h$ we use the truncated Magnus expansion,

$$u(t + h) = \mathrm{e}^{\Theta_m(t+h,t)}u(t),$$

where $\Theta_m(t + h, t)$ can be easily recovered from $\Theta_m(h, 0)$ (shortened to $\Theta_m(h)$) by substituting all occurrences of $V(\zeta)$ by $V(t + \zeta)$. Let us define the midpoint of the interval $[t, t + h]$ as $t_{1/2} = t + h/2$. Recalling that the expansion is odd about $t_{1/2}$, we shift the origin to $t_{1/2}$ by defining

$$W(\zeta) := V(t_{1/2} + \zeta),$$

whereby we need to substitute $V(\zeta)$ with $W(\zeta - h/2)$ in the Magnus expansion. Specifically, for methods described here, this only needs to be done in the terms $\mu_{j,k}(h)$ and

$\Lambda\left[f\right]_{a,b}(h)$,

$$\mu_{j,k}(h) := \int_0^h \tilde{B}_j^k(h,\zeta)\, W\left(\zeta - \frac{h}{2}\right) \mathrm{d}\zeta, \tag{3.8}$$

$$\Lambda\left[f\right]_{a,b}(h) := \int_0^h \int_0^\zeta f(h,\zeta,\xi) \left[\partial_x^a W\left(\zeta - \frac{h}{2}\right)\ \partial_x^b W\left(\xi - \frac{h}{2}\right)\right] \mathrm{d}\xi\, \mathrm{d}\zeta. \tag{3.9}$$

As we demonstrate in the rest of this section, this substitution allows us to identify and discard even-powered terms in the Magnus expansion.

Remark 10 *Since we have shifted the origin to $t_{1/2}$, all odd and even components are to be understood with respect to 0 from this point onwards. This makes identification of the odd components of the Magnus expansion simpler, assuming that the odd and even components of W can be found.*

3.4 Odd and even components of μ and Λ

Extending the new definitions of μ and Λ (3.8, 3.9), we define

$$\mu_{\star,j,k}(h) := \int_0^h \tilde{B}_j^k(h,\zeta)\, W^\star\left(\zeta - \frac{h}{2}\right) \mathrm{d}\zeta, \quad \star \in \{e,o\}, \tag{3.10}$$

and

$$\Lambda\left[f\right]_{\star,a,b}(h) := \int_0^h \int_0^\zeta f(h,\zeta,\xi) \left[\partial_x^a W\left(\zeta - \frac{h}{2}\right)\ \partial_x^b W\left(\xi - \frac{h}{2}\right)\right]^\star \mathrm{d}\xi\, \mathrm{d}\zeta, \quad \star \in \{e,o\}. \tag{3.11}$$

The even and odd components of $\mu_{j,k}(h)$ and $\Lambda\left[f\right]_{a,b}(h)$ can easily be expressed in terms of these new definitions,

$$\left(\mu_{j,k}(h)\right)^o = \begin{cases} \mu_{e,j,k}(h) & \text{if } jk \text{ is even,} \\ \mu_{o,j,k}(h) & \text{if } jk \text{ is odd,} \end{cases} \qquad \left(\mu_{j,k}(h)\right)^e = \begin{cases} \mu_{o,j,k}(h) & \text{if } jk \text{ is even,} \\ \mu_{e,j,k}(h) & \text{if } jk \text{ is odd,} \end{cases}$$

where we exploit the fact that $\tilde{B}_j(h,\zeta)$ is odd in (h,ζ) for odd values of j and even for even values. For instance, $\mu_{0,0}(h)^o = \mu_{e,0,0}(h) = \int_0^h W^e\left(\zeta - \frac{h}{2}\right) \mathrm{d}\zeta$. Note carefully the difference of usage in subscript and superscript. The odd and even parts of $\Lambda\left[f\right]_{a,b}(h)$ are

$$\Big(\Lambda\left[f\right]_{a,b}(h)\Big)^o = \Lambda\left[f^o\right]_{e,a,b}(h) + \Lambda\left[f^e\right]_{o,a,b}(h),$$
$$\Big(\Lambda\left[f\right]_{a,b}(h)\Big)^e = \Lambda\left[f^o\right]_{o,a,b}(h) + \Lambda\left[f^e\right]_{e,a,b}(h).$$

For an odd function such as $\psi(h,\zeta,\xi) := \zeta - \xi - \frac{h}{3}$, for instance, this reduces to

$$\Big(\Lambda\left[\psi\right]_{a,b}(h)\Big)^o = \Lambda\left[\psi\right]_{e,a,b}(h).$$

3.5 Expanding μ and Λ in powers of h.

A natural consequence of separating odd and even components is that the sizes of certain μ and Λ integrals become smaller (i.e. they are associated with higher powers of h) than prescribed by Lemmas 2 and 3. Essentially, this is due to certain terms disappearing in the relevant Taylor expansions.

Lemma 4 *For an analytic potential V (and thus W),*

$$\mu_{e,j,k}(h) = \mathcal{O}\left(h^{jk+1}\right), \quad k \neq 1, \qquad \mu_{e,j,1}(h) = \mathcal{O}\left(h^{j+3}\right), \tag{3.12}$$

and

$$\mu_{o,j,k}(h) = \mathcal{O}\left(h^{jk+2}\right), \quad k \geq 0. \tag{3.13}$$

Proof *For an analytic potential, $W(\zeta - h/2) = \sum_{n=0}^{\infty}[W^{(n)}(0)/n!]\,(\zeta - h/2)^n$, we expect a gain of a single power of h in $\mu_{j,1}(h)$ since $\int_0^h \tilde{B}_j(h,\zeta)W(0)\,\mathrm{d}\zeta$ vanishes (see Lemma 2). Thus, instead of being $\mathcal{O}\left(h^{j+1}\right)$, this term turns out to be $\mathcal{O}\left(h^{j+2}\right)$.*

In the case of $\mu_{e,j,1}(h)$ where we take the even part of the potential W at $\zeta - \frac{h}{2}$, we see a gain of two powers of h since the smallest non-vanishing term is

$$\frac{1}{2}\int_0^h B_j(h,\zeta)W^{(2)}(0)\left(\zeta - \frac{h}{2}\right)^2 \mathrm{d}\zeta.$$

Thus, $\mu_{e,j,1}(h) = \mathcal{O}\left(h^{j+3}\right)$ instead of being $\mathcal{O}\left(h^{j+2}\right)$. This is the only exception to Lemma 2 for $\mu_{e,j,k}(h)$. Similarly, for $\mu_{o,j,k}(h)$, observe that there is no $W^{(0)}$ term in the Taylor expansion. □

Lemma 5 *For a polynomial $r_n(h,\zeta,\xi)$ featuring only degree-n terms in h, ζ and ξ,*

$$\Lambda\left[r_n\right]_{e,1,1}(h) = \mathcal{O}\left(h^{n+2}\right), \tag{3.14}$$

while for a polynomial p_n whose integral over the triangle vanishes,

$$\int_0^h \int_0^\zeta p_n(h,\zeta,\xi)\,\mathrm{d}\xi\,\mathrm{d}\zeta = 0,$$

$$\Lambda\left[p_n\right]_{e,1,1}(h) = \mathcal{O}\left(h^{n+4}\right). \tag{3.15}$$

In particular, the exception (3.15) holds for ψ, ϕ_1 and ϕ_2, but not for φ_1 and φ_2. For the odd part,

$$\Lambda\left[r_n\right]_{o,1,1}(h) = \mathcal{O}\left(h^{n+3}\right), \tag{3.16}$$

whether the integral of r_n vanishes or not.

The proof for Lemma 5 follows directly along the lines of Lemma 4.

3.6 Identifying the odd components of Magnus expansions

Recall that the time symmetry of power truncated Magnus expansions ensures that, having shifted the origin to $t_{1/2}$, Θ_m is odd about the origin. Therefore the even part Θ_m^e vanishes, and it suffices to work with $\Theta_m = \Theta_m^o$. For the sixth-order based simplified-commutator Magnus expansion of (Iserles et al. 2018), Θ_4, we can identify the odd components using the results of Subsection 3.4,

$$\begin{aligned}\Theta_4 = \Theta_4^o = &\overbrace{\mathrm{i}h\varepsilon\partial_x^2 - \mathrm{i}\varepsilon^{-1}\mu_{e,0,0}(h)}^{\mathcal{O}\left(h\varepsilon^{-1}\right)} - \overbrace{2\left\langle\partial_x\mu_{o,1,1}(h)\right\rangle_1}^{\mathcal{O}\left(h^3\varepsilon^{-1}\right)} \\ &+ \overbrace{\mathrm{i}\varepsilon^{-1}\Lambda\left[\psi\right]_{e,1,1}(h) + 2\mathrm{i}\varepsilon\left\langle\partial_x^2\mu_{e,2,1}(h)\right\rangle_2}^{\mathcal{O}\left(h^5\varepsilon^{-1}\right)} \\ &+ \overbrace{\tfrac{1}{6}\varepsilon^{-1}\left\langle\Lambda\left[\varphi_1+\phi_1\right]_{o,1,2}(h) + \Lambda\left[\varphi_2+\phi_2\right]_{o,2,1}(h)\right\rangle_1}^{\mathcal{O}\left(h^5\varepsilon^{-1}\right)} \\ &+ \overbrace{\tfrac{4}{3}\varepsilon^2\left\langle\partial_x^3\mu_{o,3,1}(h)\right\rangle_3}^{\mathcal{O}\left(h^5\varepsilon^{-1}\right)} + \overbrace{\tfrac{1}{4}\mathrm{i}\varepsilon\partial_x^4\mu_{e,2,1}(h)}^{\mathcal{O}\left(h^5\varepsilon\right)} = \Theta(h) + \mathcal{O}\left(\varepsilon^{7\sigma-1}\right),\end{aligned} \tag{3.17}$$

where size analysis in powers of h is done using Lemmas 4 and 5, and we have used the fact that $\Big(\Lambda\left[\varphi_j+\phi_j\right]_{a,b}(h)\Big)^o = \Lambda\left[\varphi_j+\phi_j\right]_{o,a,b}(h)$, since $\varphi_j+\phi_j$ is even. We can now discard the $\mathcal{O}\left(h^5\varepsilon\right)$ term $\frac{1}{4}\mathrm{i}\varepsilon\partial_x^4\mu_{e,2,1}(h)$ since it is $\mathcal{O}\left(\varepsilon^{7\sigma-1}\right)$ or smaller under the assumption $\sigma \le 1$.

By this stage we have been able to eradicate all even powers of h and are now in a position to effectively apply the Zassenhaus splitting to the sixth-order based Magnus expansion Θ_4^o.

3.7 Symmetric Zassenhaus splitting

A Zassenhaus splitting commencing from the Magnus expansion Θ_4^o naturally yields an exponential splitting featuring only $\mathcal{O}\left(\varepsilon^{\sigma-1}\right)$, $\mathcal{O}\left(\varepsilon^{3\sigma-1}\right)$ and $\mathcal{O}\left(\varepsilon^{5\sigma-1}\right)$ terms,

$$\exp\left(\Theta_4\right) = \mathrm{e}^{\frac{1}{2}W^{[0]}}\mathrm{e}^{\frac{1}{2}W^{[1]}}\mathrm{e}^{\frac{1}{2}W^{[2]}}\mathrm{e}^{\mathcal{W}^{[3]}}\mathrm{e}^{\frac{1}{2}W^{[2]}}\mathrm{e}^{\frac{1}{2}W^{[1]}}\mathrm{e}^{\frac{1}{2}W^{[0]}} + \mathcal{O}\left(\varepsilon^{7\sigma-1}\right), \tag{3.18}$$

where

$$
\begin{aligned}
W^{[0]} &= \mathrm{i}h\varepsilon\partial_x^2 = \mathcal{O}\left(\varepsilon^{\sigma-1}\right),\\
W^{[1]} &= -\mathrm{i}\varepsilon^{-1}\mu_{e,0,0}(h) = \mathcal{O}\left(\varepsilon^{\sigma-1}\right),\\
W^{[2]} &= \tfrac{1}{6}\mathrm{i}h\varepsilon^{-1}\left(\partial_x\mu_{e,0,0}(h)\right)^2 - 2\left\langle\partial_x\mu_{o,1,1}(h)\right\rangle_1 + \tfrac{1}{6}\mathrm{i}h^2\varepsilon\left\langle\partial_x^2\mu_{e,0,0}(h)\right\rangle_2 = \mathcal{O}\left(\varepsilon^{3\sigma-1}\right),\\
\mathcal{W}^{[3]} &= \mathrm{i}\varepsilon^{-1}\Lambda\left[\psi\right]_{e,1,1}(h) - \tfrac{1}{24}\mathrm{i}h^2\varepsilon\left(\partial_x^4\mu_{e,0,0}(h)\right) - \tfrac{1}{6}\mathrm{i}\varepsilon^{-1}\left(\partial_x\mu_{e,0,0}(h)\right)^2\left(\partial_x^2\mu_{e,2,1}(h)\right)\\
&\quad - \tfrac{2}{45}\mathrm{i}h^2\varepsilon^{-1}\left(\partial_x\mu_{e,0,0}(h)\right)^2\left(\partial_x^2\mu_{e,0,0}(h)\right)\\
&\quad + \tfrac{1}{6}\left\langle\Lambda\left[\varphi_1+\phi_1\right]_{o,1,2}(h) + \Lambda\left[\varphi_2+\phi_2\right]_{o,2,1}(h)\right\rangle_1\\
&\quad - h\left\langle\left(\partial_x\mu_{e,0,0}(h)\right)\left(\partial_x^2\mu_{o,1,1}(h)\right) - \tfrac{1}{3}\left(\partial_x^2\mu_{e,0,0}(h)\right)\left(\partial_x\mu_{o,1,1}(h)\right)\right\rangle_1\\
&\quad + \tfrac{1}{30}\mathrm{i}h^3\varepsilon\left\langle\left(\partial_x^2\mu_{e,0,0}(h)\right)^2 - 2\left(\partial_x\mu_{e,0,0}(h)\right)\left(\partial_x^3\mu_{e,0,0}(h)\right)\right\rangle_2\\
&\quad + 2\mathrm{i}\varepsilon\left\langle\partial_x^2\mu_{e,2,1}(h)\right\rangle_2 + \tfrac{4}{3}\varepsilon^2\left\langle\partial_x^3\mu_{o,3,1}(h)\right\rangle_3\\
&\quad + \tfrac{1}{3}h^2\varepsilon^2\left\langle\partial_x^3\mu_{o,1,1}(h)\right\rangle_3 - \tfrac{1}{120}\mathrm{i}h^4\varepsilon^3\left\langle\partial_x^4\mu_{e,0,0}(h)\right\rangle_4 = \mathcal{O}\left(\varepsilon^{5\sigma-1}\right),
\end{aligned}
$$

The term $\frac{1}{24}\mathrm{i}h^2\varepsilon\left(\partial_x^4\mu_{e,0,0}(h)\right)$ in $\mathcal{W}^{[3]}$ is $\mathcal{O}\left(\varepsilon^{3\sigma+1}\right)$. We remind the reader that this splitting is obtained subject to $\sigma \le 1$. For $1/2 < \sigma \le 1$, this term can be combined with the $\mathcal{O}\left(\varepsilon^{5\sigma-1}\right)$ terms in $\mathcal{W}^{[3]}$, whereas for $\sigma \le 1/2$ it can be ignored since it is smaller than $\mathcal{O}\left(\varepsilon^{7\sigma-1}\right)$.

3.8 Remarks concerning implementation

The approximation of the exponentials in (3.18) can be done along the same lines as Subsection 2.4. For instance, for $h = \mathcal{O}\left(\varepsilon^{1/2}\right)$, the exponents $W^{[2]}$ and $\mathcal{W}^{[3]}$ are $\mathcal{O}\left(\varepsilon^{1/2}\right)$ and $\mathcal{O}\left(\varepsilon^{3/2}\right)$, respectively. Approximating their exponentials to an accuracy of $\mathcal{O}\left(\varepsilon^{7\sigma-1}\right) = \mathcal{O}\left(\varepsilon^{5/2}\right)$ requires five and two Lanczos iterations, respectively. Each Lanczos iteration requires the computation of a matrix–vector product via (2.17).

Using the strategy (2.17), the FFTs are combined so that the computation of $\widetilde{\mathcal{W}^{[2]}}\boldsymbol{v}$ in each Lanczos iteration requires six FFTs once again, while $\widetilde{\mathcal{W}^{[3]}}\boldsymbol{v}$ requires ten FFTs. For $\sigma = 1/2$, we need $2\times5\times6 = 60$ FFTs for the exponentiation of the two occurrences of $\mathcal{W}^{[2]}$ and $1\times2\times10 = 20$ for $\mathcal{W}^{[3]}$. The total number of FFTs in a single step is 84 under $\sigma = 1/2$, after accounting for two occurrences of $\mathcal{W}^{[0]}$. Under $\sigma = 1$, the number of FFTs required reduces to $2\times3\times6 + 1\times2\times10 + 2\times2 = 60$ since the number of Lanczos iterations required are three for $\mathcal{W}^{[2]}$ and two for $\mathcal{W}^{[3]}$ (Bader et al. 2014). This is less than the case of $\sigma = 1/2$. Note, however, that the number of time steps required for integration to time T under $\sigma = 1/2$ is $\mathcal{O}\left(T/\sqrt{\varepsilon}\right)$, which makes the method less costly than under $\sigma = 1$, where the number of steps is $\mathcal{O}\left(T/\varepsilon\right)$.

In each time step of the order-six based scheme (3.18), we need to approximate five line integrals ($\mu_{e,0,0}(h)$, $\mu_{o,1,1}(h)$, $\mu_{e,1,2}(h)$, $\mu_{e,2,1}(h)$, $\mu_{o,3,1}(h)$) and three integrals over the triangle ($\Lambda\left[\phi\right]_{e,1,1}(h)$, $\Lambda\left[\psi_1+\theta_1\right]_{o,1,2}(h)$ and $\Lambda\left[\psi_2+\theta_2\right]_{o,2,1}(h)$). If analytic expressions are not available, it is possible to approximate these through quadrature formulae such as Gauss–Legendre quadrature. For the $\mathcal{O}\left(\varepsilon^{7\sigma-1}\right)$ splitting here, for

instance, we require merely three Gauss–Legendre knots $t_k = h(1 + k\sqrt{3/5})/2, k = -1, 0, 1$, with weights $w_k = \frac{5}{18}h, \frac{4}{9}h, \frac{5}{18}h$ (Davis & Rabinowitz 1984), respectively, for the $\mathcal{O}\left(h^7\right)$ accuracy which is required of the quadrature.

Evaluation for the integrals over the line, $\mu_{\star,j,k}(h)$, follows directly using these quadrature knots. Integrals over the triangle are also easily evaluated using the same three knots by substituting W with its interpolating polynomial. A more detailed narrative on the approximation of such integrals can be found in (Iserles et al. 2018).

4 Numerical examples

In this section we will present one, two and three-dimensional examples ($d = 1, 2, 3$) with a Gaussian wavepacket centred at $\mathbf{x}_0 \in \mathbb{R}^d$ with spread δ,

$$u_{0,d}(\mathbf{x}) = (\delta\pi)^{-d/4} \exp\left(-(\mathbf{x} - \mathbf{x}_0)^2/(2\delta)\right),$$

as the initial condition.

4.1 One-dimensional double well.

For our first numerical experiment we consider a one-dimensional ($d = 1$) Gaussian wavepacket with $x_0 = -2.5$ and $\delta = 10^{-2}$, sitting in the left well of a double well potential,

$$V_{\mathrm{D1}}(x) = \tfrac{1}{5}x^4 - 2x^2.$$

We take $[-5, 5]$ as our spatial domain and $[0, \frac{5}{2}]$ as our temporal domain. In the first instance, we consider the behaviour subject to $\varepsilon = 10^{-2}$. When we allow the wave function $u_{0,1}$ to evolve to $u_{\mathrm{D},1}(T)$ under the influence of V_{D1} alone, it remains largely confined to the left well at the final time, $T = \frac{5}{2}$ (Figure 4.1, left).

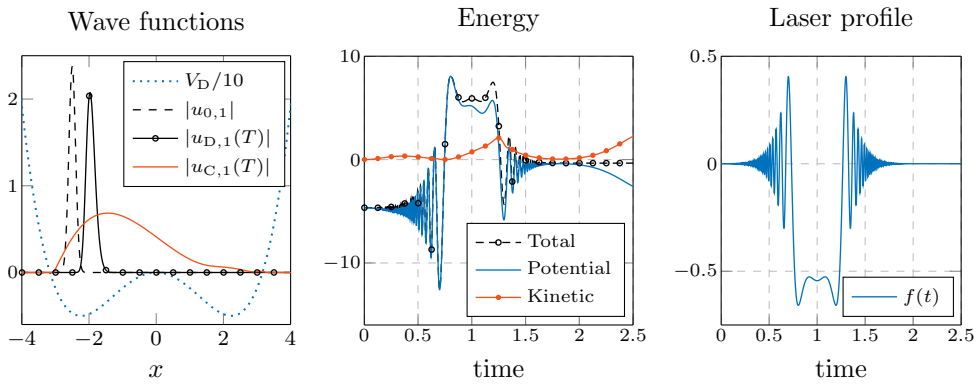

Figure 4.1: The initial condition $u_{0,1}$ evolves to $u_{\mathrm{D},1}$ under the influence of V_{D1} and to $u_{\mathrm{C},1}$ under V_{C1} (left); Evolution of energy under V_{C1} (centre); Laser profile $f(t)$ (right). Here, the semiclassical parameter is $\varepsilon = 10^{-2}$ and the potential V_{D1} is scaled down for ease of presentation.

Time-dependent potential. Adding a time dependent excitation of the form $f(t)\,x$ on the potential – used for modeling laser interaction – we are able to exert control on the wave function. The time profile of the laser used here is

$$f(t) = \exp(-10(t-1)^2)\sin((500(t-1)^4 + 10)),$$

which is a highly oscillatory function (Figure 4.1, right). Electric fields of this form, where the instantaneous frequency changes, are called *chirped* pulses. These are used routinely in laser control (Amstrup, Doll, Sauerbrey, Szabó & Lorincz 1993). Even more oscillatory electric fields often result from optimal control algorithms (Meyer, Wang & May 2006, Coudert 2018).

The effective time-dependent potential is

$$V_{\mathrm{C1}}(x,t) = V_{\mathrm{D1}}(x) + 10f(t)x.$$

Under the influence of the time-dependent potential $V_{\mathrm{C1}}(x,t)$, the initial wave-function u_0 evolves to $u_{\mathrm{C},1}(T)$, which is not confined to the left well (Figure 4.1, left). In this case, the total energy is not conserved, stabilising at a higher level once the external influence vanishes (Figure 4.1, centre).

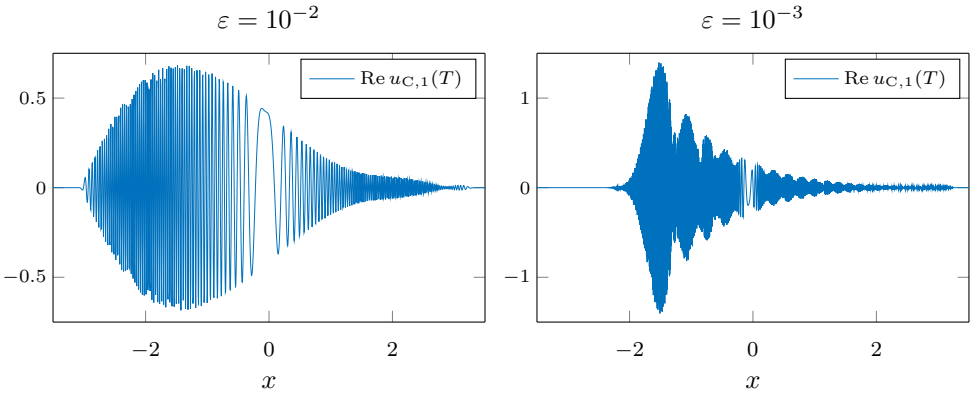

Figure 4.2: The highly oscillatory nature of the wavefunction for $\varepsilon = 10^{-2}$ and 10^{-3} is evident in the phase.

4.2 Higher dimensions.

The second and third examples generalise the first example to two and three dimensions, respectively. We consider the evolution of the Gaussian wavepackets $u_{0,2}(\mathbf{x})$ sitting at $\mathbf{x}_0 = (-0.5, 0)$ and $u_{0,3}(\mathbf{x})$ sitting at $\mathbf{x}_0 = (-0.5, 0, 0)$ in the left wells of the potentials,

$$V_{\mathrm{D2}}(\mathbf{x}) = ((x-0.5)^2 + y^2)((x+0.5)^2 + y^2)$$

and

$$V_{\mathrm{D3}}(\mathbf{x}) = ((x-0.5)^2 + y^2 + z^2)((x+0.5)^2 + y^2 + z^2),$$

respectively. The time-dependent potentials used are

$$V_{\mathrm{C}2}(\mathbf{x},t) = V_{\mathrm{D}2}(\mathbf{x}) + f(t)x \quad \text{and} \quad V_{\mathrm{C}3}(\mathbf{x},t) = V_{\mathrm{D}3}(\mathbf{x}) + f(t)x,$$

respectively.

Here we consider the behaviour under $\varepsilon = 1/250$ and the spread of the wavepackets is taken to be $\delta = \varepsilon$ again. The spatial domain is $[-2,2]\times[-2,2]$ in two dimensions and $[-1.5,1.5]\times[-1,1]\times[-1,1]$ in three dimensions, while the temporal domain remains $[0,\frac{5}{2}]$.

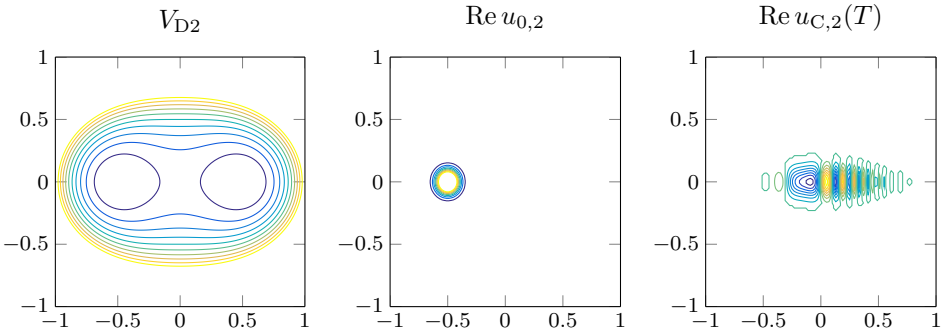

Figure 4.3: The double-well potential $V_{\mathrm{D}2}$ in two dimensions shown with contour lines from level 0 up to 0.5, each separated by 0.05 (left); initial condition $u_{0,2}$ (centre) evolves to to $u_{\mathrm{C},2}(T)$ (right) under the influence of $V_{\mathrm{C}2}$, with contour lines ranging from level -4 to 4, separated by 0.5. Here, the semiclassical parameter is $\varepsilon = 1/250$.

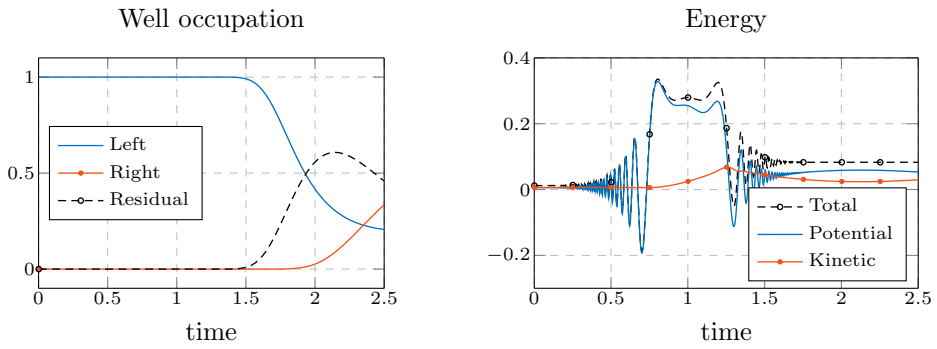

Figure 4.4: Probability of particle being in the two wells in three dimensions under $V_{\mathrm{C}3}$ (left); evolution of energy (right). Here, $\varepsilon = 1/250$.

In three dimensions the movement of the wavefunction from the left to the right well is visible in Figure 4.4 (left) which shows the probability of the particle being in the two wells. The probability of the particle being in an area A is given by

$$P_A(t) = \|\chi_A u(t)\|_2^2,$$

where χ_A is the indicator (or characteristic) function of the set A. The target area of the two wells is set to a radius of 0.4 from the centres ($(-0.5, 0, 0)$ for the left well and $(0.5, 0, 0)$ for the right well). The residual is defined as $P_{\text{residual}}(t) = 1 - P_{\text{left}}(t) - P_{\text{right}}(t)$.

4.3 Methods

We will use IKS4 and IKS6 to refer to the new fourth and sixth-order based methods, (1.5) and (3.18), respectively, presented in this paper. We expect the asymptotic nature of our splitting (3.18) to outperform methods based on Lanczos exponentiation of Hamiltonians (or its perturbations) due the growth of spectral radius in the semiclassical regime. For demonstrating this, we compare the accuracy and cost of our method with the sixth-order optimised method CF6:5Opt proposed in (Alvermann & Fehske 2011), labeled as AF6 in this section. This is a Lanczos-based method which is highly effective in the atomic regime ($\varepsilon = 1$). However, it is not specialised for the semiclassical regime. We also contrast the accuracy of our method to a method specialised for the semiclassical regime – the sixth-order method of (Bader et al. 2016), labeled as BIKS6 in this section. However, this method is not designed for handling highly oscillatory potentials.

Lanczos iterations. AF6 is accompanied by a postfix which refers to the number of Lanczos iterations (10, 25 or 50) used in the method. In all cases presented here, IKS6 and BIKS6 utilise two Lanczos iterations for the exponentiation of $\mathcal{W}^{[3]}$. Three Lanczos iterations are used for the exponentiation of $W^{[2]}$ in experiments where time-steps tend to be small (Figure 4.5, Figure 4.7 (left)) and five iterations are used once large time-steps are involved (Table 4.1 and Figure 4.7 (right)). These methods are accompanied by a postfix L[n_2,n_3], where n_2 and n_3 specify the number of Lanczos iterations used for $W^{[2]}$ and $\mathcal{W}^{[3]}$, respectively.

Quadrature. In all cases presented, the integrals in IKS4 (1.5) and IKS6 (3.18) are discretised via eleven Gauss–Legendre knots. In principle we can also use analytic or asymptotic approximations, as well as highly oscillatory quadrature for the integrals. Note that BIKS6 and AF6 use a fixed number of Gauss–Legendre knots – three and four, respectively.

Optimisations. Since the potentials are available in their analytic form, we use analytic derivatives in our implementation. We also exploit the special form of the potential to speed-up computations further without affecting accuracy. In particular, for a potential of the form $V_{\text{D1}}(x) + f(t)x$, where time dependence is scalar, the integrals $\mu_{\star,j,k}(h)$ and $\Lambda[f]_{\star,a,b}(h)$ can be reduced to a scalar form, the spatial derivatives do not have be computed at each step and certain terms such as $\partial_x^2\mu_{o,1,1}(h), \partial_x^3\mu_{o,1,1}(h), \partial_x^2\mu_{e,2,1}(h)$ and $\partial_x^3\mu_{o,3,1}(h)$ vanish. Relevant optimisation steps are applied to all methods under consideration.

4.4 Numerical results

Large time steps. From Table 4.1 we can see that BIKS and AF6 L50 do not provide physically meaningful solutions when the time step h is larger than ε. This is due to the poor resolution of the highly oscillatory potential. In the case of AF6 L50, the large number of Lanczos iterations required when using large-time steps is also a very

N		30	40	50	60	75	100
h		0.083	0.063	0.050	0.042	0.033	0.025
	IKS6 L[5,2]	0.4967	0.3937	0.1606	0.0447	0.0021	0.0004
L^2	BIKS6 L[5,2]	1.3855	1.3971	1.2943	0.7883	1.8290	0.3783
error	AF6 L50	1.4148	1.4143	1.4144	1.4132	1.4020	0.3513
Error	IKS6 L[5,2]	0.1609	0.0012	0.0012	0.00046	0.000016	0.000001
in	BIKS6 L[5,2]	4.0501	11.420	15.620	0.98735	0.332851	0.000536
energy	AF6 L50	11.686	9.2533	10.183	7.36785	11.23268	0.003209
	IKS6 L[5,2]	0.44	0.56	0.74	0.77	0.90	1.25
Cost	BIKS6 L[5,2]	0.42	0.53	0.64	0.74	0.92	1.19
(s)	AF6 L50	2.63	3.47	4.33	5.20	6.39	8.45

Table 4.1: Juxtaposition of L^2 error, error in total energy (an observable) and cost in seconds of analysed methods for relatively large time steps, h, for the one-dimensional example under $\varepsilon = 10^{-2}$. Here N is the number of time steps ($h = T/N$). The number of spatial grid points is chosen to be $M = 1000$. Here IKS6 is the proposed sixth-order based method (3.18), BIKS6 is the method presented in (Bader et al. 2016) and AF6 is CF6:5Opt from (Alvermann & Fehske 2011).

important factor in cost *vs* accuracy considerations. Due to the discretisation of the integrals in IKS6 via eleven Gauss-Legendre knots and the separation of scales in the asymptotic splitting (3.18), it behaves exceptionally well for much larger time steps, requiring very few Lanczos iterations for achieving this accuracy.

Small time steps. Having shown that IKS6 method works very well for large time steps, in Figure 4.5 we consider the case of smaller time steps, presenting two cases, with $M = 1000$ and $M = 2000$ spatial grid points. The first two columns of Figure 4.5 presents the accuracy. Once again, IKS6 seems to have significantly better accuracy than BIKS6 (not specialised for highly oscillatory potentials) and AF6 L10, AF6 L25 and AF6 L50 (not specialised for semiclassical regime). The third and fourth columns present the efficiency (accuracy *vs* cost) of methods. IKS6 is not only more accurate, but far less costly.

Note that in the case of $M = 1000$, although we achieve a high accuracy in total energy ($\sim 10^{-9}$), the accuracy in L^2 norm saturates at a relatively low level ($\sim 10^{-6}$). This is inevitable since the space resolution becomes inadequate beyond this stage. Analysing the same behaviour for $M = 2000$ (columns 2 and 4 of Figure 4.5) we observe accuracy of $\sim 10^{-9}$ both in terms of total energy and L^2 norm.

Higher dimensions. Figure 4.6 shows that similar observations hold in the case of two and three dimensional examples. Note that here we compare the sixth-order method AF6 against the fourth-order based method (1.5) developed in subsection 2.5. It is no surprise that the sixth-order AF6 exceeds the accuracy of the fourth-order method as time step becomes smaller – both, on account of the asymptotic error decrease and the superlinear accuracy of the Lanczos iterations. As evident from the accuracy vs cost plots (the third and fourth columns of Figure 4.6), however, this accuracy comes at a large cost and the fourth-order method (1.5) is significantly more efficient. Thus, if very high accuracy is desired and computational time is not a significant constraint, Lanczos based methods perform exceptionally well. As seen

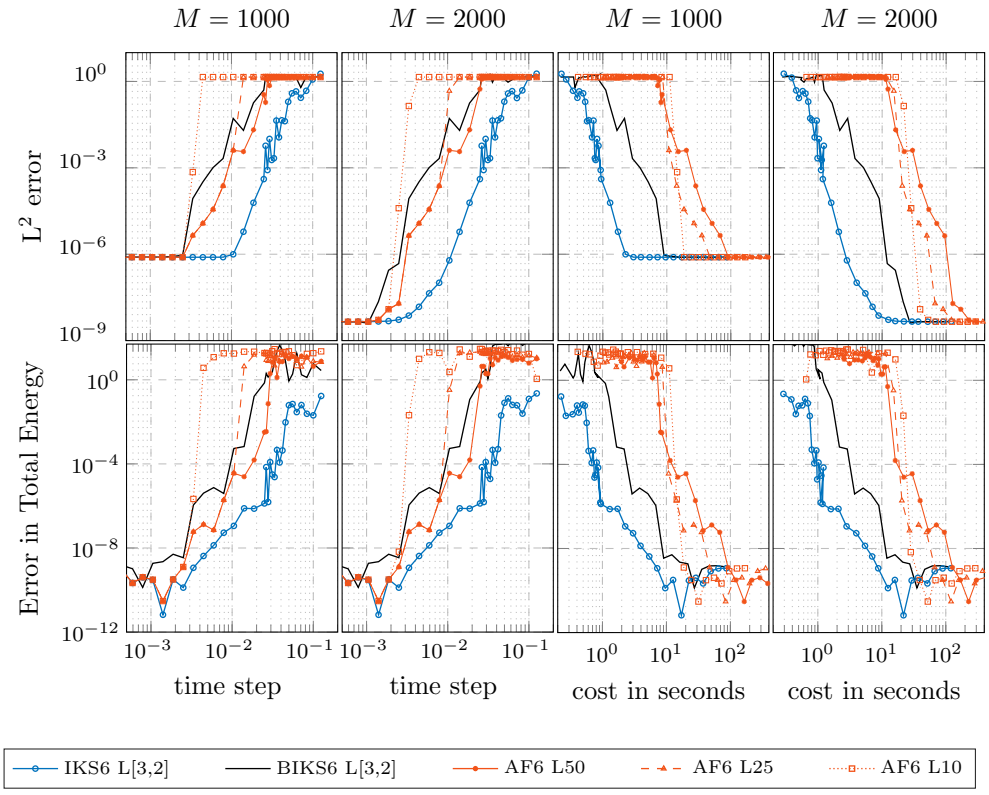

Figure 4.5: L^2 error (top row) and error in the total energy (bottom row) for the one-dimensional example under $\varepsilon = 10^{-2}$. First two columns present accuracy *vs* time step for $M = 1000$ spatial grid points and $M = 2000$ spatial grid points, respectively. The two subsequent columns illustrate the accuracy *vs* cost in seconds. Here IKS6 is the proposed sixth-order based method (3.18), BIKS6 is the method presented in (Bader et al. 2016) and AF6 is CF6:5Opt from (Alvermann & Fehske 2011).

in the one dimensional case, the proposed methods hold a significant advantage when large time steps are required and computational cost is a constraint.

Semiclassical regime. As the semiclassical parameter ε becomes smaller, the effects discussed above become more pronounced. In particular, choosing a time step as small or smaller than ε becomes infeasible. As we seek larger time-steps, such as $h = \sqrt{\varepsilon}/2$ used in Figure 4.7 (right), for instance, AF6 L50 and BIKS6 are not able to attain any meaningful accuracy, in contrast to the presented method.

Reference solutions. The reference solutions for these experiments were generated by using the sixth-order schemes BIKS6 and AF6 L10 with very small time steps. In the case of $\varepsilon = 10^{-2}$ experiments, we use $M = 5000$ grid points and $h = 2.5 \times 10^{-6}$ as time step, which corresponds to $N = 10^6$ time steps. For Figure 4.7, where ε is varied, we use BIKS6 for generating reference solutions, using $M = \lceil 20/\varepsilon \rceil$ spatial

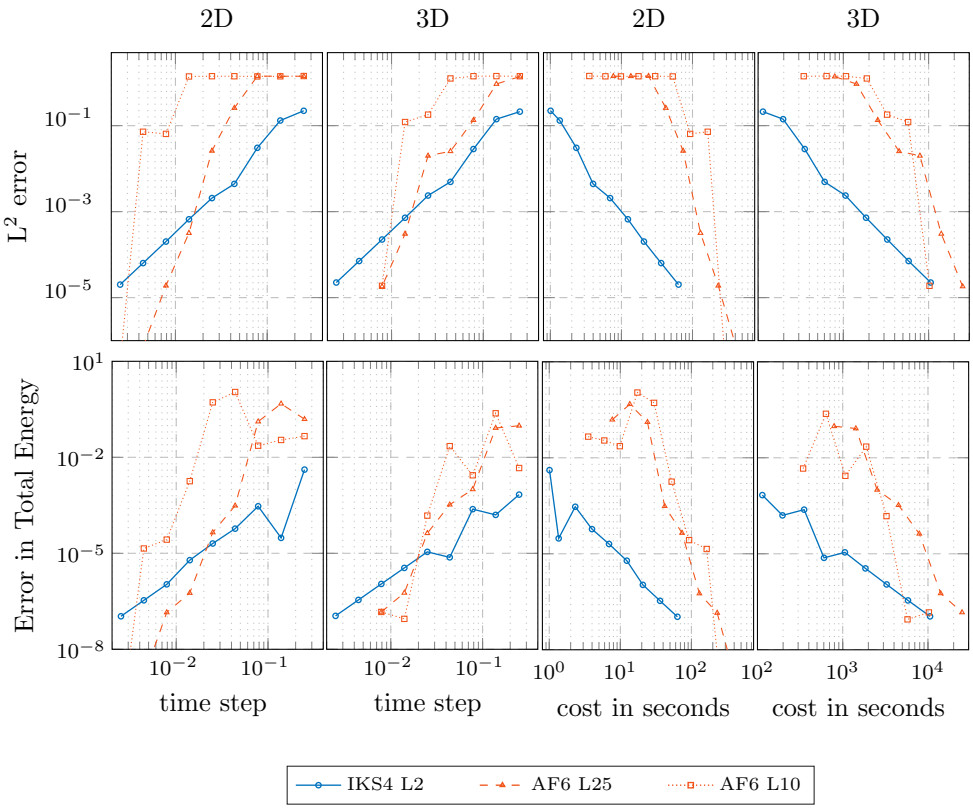

Figure 4.6: L^2 error (top row) and error in the total energy (bottom row) for two and three-dimensional examples under $\varepsilon = 1/250$. First two columns present accuracy *vs* time step for the two dimensional example and the three dimensional example, respectively. The two subsequent columns illustrate the accuracy *vs* cost in seconds. Here IKS4 is the proposed fourth-order based method (1.5) and AF6 is the sixth-order method CF6:5Opt from (Alvermann & Fehske 2011).

grid points.

5 Conclusions

To conclude, in this paper we have introduced a new numerical approach for the approximation of Schrödinger equation in semiclassical regime. This methodology is especially powerful in the case of highly oscillatory, time-dependent potentials. We have outlined a procedure for deriving arbitrarily high-accuracy numerical schemes, and have presented second, fourth and sixth order based schemes of this class of methods, which feature a global accuracy of $\mathcal{O}\left(\varepsilon^{2\sigma-1}\right), \mathcal{O}\left(\varepsilon^{4\sigma-1}\right)$ and $\mathcal{O}\left(\varepsilon^{6\sigma-1}\right)$, respectively.

As demonstrated with the help of numerical examples, these schemes are more

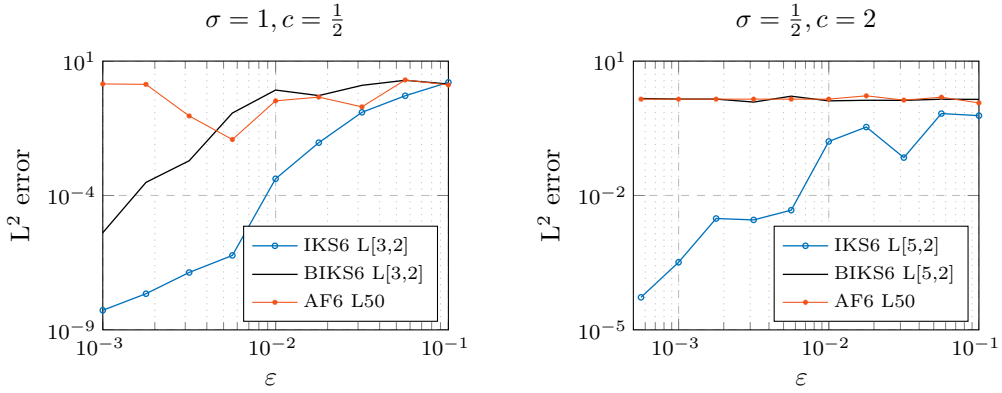

Figure 4.7: Global L^2 errors for the one-dimensional example under the time-step scaling $h = \varepsilon^\sigma/c$ with $\sigma = 1$, $c = \frac{1}{2}$ and $M = \lceil 20/\varepsilon \rceil$ spatial grid points (left) and $\sigma = \frac{1}{2}$, $c = 2$ and $M = \lceil 10/\varepsilon \rceil$ spatial grid points (right). Here IKS6 is the proposed sixth-order based method (3.18), BIKS6 is the method presented in (Bader et al. 2016) and AF6 is CF6:5Opt from (Alvermann & Fehske 2011).

effective in the semiclassical regime than

1. methods based on direct exponentiation via Lanczos iterations, which are costly in the semiclassical regime, and

2. the asymptotic Magnus–Zassenhaus splittings presented in (Bader et al. 2016), which are specialised for the semiclassical regime, once the potential features rapid temporal oscillations.

Let us briefly summarise the reason for the effectiveness of the current method in the regime under consideration. In the semiclassical regime, a decreasing ε results in increasing oscillations in both space and time, consequently requiring an increase in the resolution of spatial and temporal grids. Additionally, the highly oscillatory potential requires high temporal grid resolution.

1. All methods compared in this paper require a very fine spatial grid in the semiclassical regime. The consequent imposition of a fine temporal grid in the case of exponential propagators, however, can be seen to arise from an interplay between the growth of the spectral radius (due to a fine spatial grid) and the need to keep Lanczos iterations small. In this case, resorting to an asymptotic splitting such as the symmetric Zassenhaus splitting of (Bader et al. 2014) and (Bader et al. 2016) allows us to separate the large scales dominating the spectral radius, whereby the only terms requiring exponentiation via Lanczos iterations are asymptotically small (in increasing powers of ε) and impose considerably more relaxed constraints on the time step.

2. By preserving integrals till the very last stage, the new method decouples the task of approximating the integrals of the potential from the task of approximating the time evolution of the solution. Thus, it allows us to resort to higher

accuracy or specialised quadrature methods for the approximation of the integrals of the potential, $V(\mathbf{x}, t)$, without affecting the time step of the scheme. This is particularly effective in applications where the time-dependent part of the potential is oscillatory but not excessively expensive to evaluate, even if the time-independent part is. In all other known methods (including (Bader et al. 2016)), highly oscillatory potentials require a very high resolution in time since the sampling of the potential (via quadrature methods or otherwise) is fixed at the outset and linked to the time-propagation.

It goes without saying that, like in virtually every mathematical paper, our exposition is incomplete. In particular, no attempt has been made in this paper to optimise the performance of the Magnus–Zassenhaus approach or to exploit serendipitous connections among the terms *á la* (Blanes, Casas & Ros 2000) to reduce the cost further. This will be matter for future research.

Acknowledgments

The work of Karolina Kropielnicka in this project was financed by The National Center for Science, based on grant no. 2016/22/M/ST1/00257.

References

Abramowitz, M. & Stegun, I. A. (1964), *Handbook of Mathematical Functions with Formulas, Graphs, and Mathematical Tables*, ninth Dover printing, 10th GPO printing edn, Dover, New York.

Agueny, H., Chovancova, M., Hansen, J. P. & Kocbach, L. (2016), 'Scaling properties of field ionization of Rydberg atoms in single-cycle THz pulses: 1d considerations', *J. Phys. B: At. Mol. Opt. Phys.* **49**, 245002.

Alvermann, A. & Fehske, H. (2011), 'High-order commutator-free exponential time-propagation of driven quantum systems', *J. Comput. Phys.* **230**(15), 5930–5956.

Amstrup, B., Doll, J. D., Sauerbrey, R. A., Szabó, G. & Lorincz, A. (1993), 'Optimal control of quantum systems by chirped pulses', *Phys. Rev. A* **48**(5), 3830–3836.

Bader, P., Iserles, A., Kropielnicka, K. & Singh, P. (2014), 'Effective approximation for the semiclassical Schrödinger equation', *Found. Comput. Math.* **14**, 689–720.

Bader, P., Iserles, A., Kropielnicka, K. & Singh, P. (2016), 'Efficient methods for linear Schrödinger equation in the semiclassical regime with time-dependent potential', *Proc. A.* **472**(2193), 20150733, 18.

Bao, W., Jin, S. & Markowich, P. A. (2002), 'On time-splitting spectral approximations for the Schrödinger equation in the semiclassical regime', *J. Comput. Phys.* **175**, 487–524.

Blanes, S., Casas, F. & Murua, A. (2017*a*), 'Symplectic time-average propagators for the Schrödinger equation with a time-dependent Hamiltonian', *J. Chem. Phys.* **146**(11), 114109.

Blanes, S., Casas, F. & Ros, J. (2000), 'Improved high order integrators based on the Magnus expansion', *BIT* **40**(3), 434–450.

Blanes, S., Casas, F. & Thalhammer, M. (2017*b*), 'High-order commutator-free quasi-Magnus exponential integrators for non-autonomouslinear evolution equations', *Comput. Phys. Commun.* **220**, 243 – 262.

Blanes, S., Casas, F., Oteo, J. A. & Ros, J. (2009), 'The Magnus expansion and some of its applications', *Phys. Rep.* **470**, 151–238.

Casas, F. & Murua, A. (2009), 'An efficient algorithm for computing the Baker-Campbell-Hausdorff series and some of its applications', *J. Math. Phys.* **50**(3), 033513, 23.

Coudert, L. H. (2018), 'Optimal control of the orientation and alignment of an asymmetric-top molecule with terahertz and laser pulses', *J. Chem. Phys.* **148**(9), 094306.

Davis, P. J. & Rabinowitz, P. (1984), *Methods of Numerical Integration*, 2nd edn, Academic Press, Orlando, FL.

Hochbruck, M. & Lubich, C. (1997), 'On Krylov subspace approximations to the matrix exponential operator', *SIAM J. Numer. Anal.* **34**, 1911–1925.

Iserles, A., Kropielnicka, K. & Singh, P. (2018), 'Magnus–Lanczos methods with simplified commutators for the Schrödinger equation with a time-dependent potential', *Submitted*.

Iserles, A., Munthe-Kaas, H. Z., Nørsett, S. P. & Zanna, A. (2000), 'Lie-group methods', *Acta Numerica* **9**, 215–365.

Iserles, A., Nørsett, S. P. & Rasmussen, A. (2001), 'Time symmetry and high-order Magnus methods', *Appl. Numer. Math.* **39**(3–4), 379–401.

Jin, S., Markowich, P. & Sparber, C. (2011), 'Mathematical and computational methods for semiclassical Schrödinger equations', *Acta Numerica* **20**, 121–210.

Lehmer, D. H. (1988), 'A new approach to Bernoulli polynomials', *Am. Math. Monthly* **95**(10), 905–911.

Lubich, C. (2008), *From Quantum to Classical Molecular Dynamics: Reduced Models and Numerical Analysis*, Zurich Lectures in Advanced Mathematics, Europ. Math. Soc., Zürich.

Magnus, W. (1954), 'On the exponential solution of differential equations for a linear operator', *Comm. Pure Appl. Math.* **7**, 649–673.

Meyer, H., Wang, L. & May, V. (2006), Optimal control of multidimensional vibronic dynamics: Algorithmic developments and applications to 4d-Pyrazine, *in* B. Lasorne & G. A. Worth, eds, 'Proceedings of the CCP6 workshop on Coherent Control of Molecules', CCP6, pp. 50–55.

Munthe-Kaas, H. & Owren, B. (1999), 'Computations in a free Lie algebra', *Phil. Trans. Royal Soc. A* **357**(1754), 957–981.

Murua, A. (2010), 'The symmetric Baker–Campbell–Hausdorff formula up to terms of degree 20 written in a Hall basis or a Lyndon basis', `http://www.ehu.es/ccwmuura/research/sbchHall19.dat`.

Ndong, M., Tal-Ezer, H., Kosloff, R. & Koch, C. P. (2010), 'A Chebychev propagator with iterative time ordering for explicitly time-dependent Hamiltonians', *J. Chem. Phys.* **132**(6), 064105.

Peskin, U., Kosloff, R. & Moiseyev, N. (1994), 'The solution of the time dependent Schrödinger equation by the (t,t) method: The use of global polynomial propagators for time dependent Hamiltonians', *J. Chem. Phys.* **100**(12), 8849–8855.

Reutenauer, C. (1993), *Free Lie Algebras*, London Maths Soc. Monographs **7**, Oxford University Press, Oxford.

Sanz-Serna, J. M. & Portillo, A. (1996), 'Classical numerical integrators for wavepacket dynamics', *J. Chem. Phys.* **104**(6), 2349–2355.

Schaefer, I., Tal-Ezer, H. & Kosloff, R. (2017), 'Semi-global approach for propagation of the time-dependent Schrödinger equation for time-dependent and nonlinear problems', *J. Comput. Phys.* **343**, 368–413.

Singh, P. (2015), Algebraic theory for higher order methods in computational quantum mechanics, arXiv:1510.06896 [math.NA].

Singh, P. (2017), High accuracy computational methods for the semiclassical Schrödinger equation, PhD thesis, University of Cambridge.

Tal-Ezer, H., Kosloff, R. & Cerjan, C. (1992), 'Low-order polynomial approximation of propagators for the time-dependent Schrödinger equation', *J. Comput. Phys.* **100**(1), 179–187.

Tremblay, J. C. & Carrington Jr., T. (2004), 'Using preconditioned adaptive step size Runge–Kutta methods for solving the time-dependent Schrödinger equation', *J. Chem. Phys.* **121**(23), 11535–11541.

A The algebra of anti-commutators

The vector field of the Schrödinger equation (1.1) is a linear combination of the action of two operators, ∂_x^2 and the multiplication by the interaction potential $V(t)$, for any

$t \geq 0$. Since the Magnus expansion requires nested commutation, the focus of our interest is the Lie algebra generated by ∂_x^2 and $V(\cdot)$,

$$\mathfrak{F} = \mathrm{LA}\{\partial_x^2, V(\cdot)\},$$

i.e. the linear-space closure of all nested commutators of ∂_x^2 and $V(\cdot)$.

Simplifying commutators. To simplify commutators we could study their action on functions. For example, using the chain rule we find,

$$[\partial_x^2, V]u = \partial_x^2(Vu) - V(\partial_x^2 u) = (\partial_x^2 V)u + 2(\partial_x V)\partial_x u,$$

which implies that $[\partial_x^2, V] = (\partial_x^2 V) + 2(\partial_x V)\partial_x$. Straightforward discretisation of these simplified commutators,

$$(\partial_x^2 V) + 2(\partial_x V)\partial_x \rightsquigarrow \mathcal{D}_{(\partial_x^2 V)} + 2\mathcal{D}_{(\partial_x V)}\mathcal{K}_1,$$

are not skew-Hermitian (or even Hermitian, for that matter). In practice, this results in a loss of unitarity and stability when such matrices are exponentiated.

In the methods presented here we circumvent the problem by working with *anti-commutators*, that is the differential operators of the form (2.3),

$$\langle f \rangle_k := \tfrac{1}{2}\left(f \circ \partial_x^k + \partial_x^k \circ f\right), \quad k \geq 0,\ f \in \mathrm{C}_p^\infty(I;\mathbb{R}),$$

which are inherently symmetrised. The action of this differential operator on u, for example, is

$$\langle f \rangle_k u = \tfrac{1}{2}\left(f\partial_x^k u + \partial_x^k(fu)\right)$$

and the discretisation of this operator, given by (2.4), is

$$\langle f \rangle_k \rightsquigarrow \tfrac{1}{2}\left(\mathcal{D}_f\mathcal{K}_k + \mathcal{K}_k\mathcal{D}_f\right).$$

It is simple matter to verify that the discretisation of $\langle f \rangle_k$ is skew-Hermitian for odd k and Hermitian for even k. This is the reason why the choice of algebra of anti-commutators $\langle\cdot\rangle_k$ seems to be optimal for our purposes.

Moreover, the commutators of these symmetrised differential operators can be simplified using the following rules,

$$\begin{aligned}
&[\langle f\rangle_1, \langle g\rangle_0] = \langle f(\partial_x g)\rangle_0, \\
&[\langle f\rangle_1, \langle g\rangle_1] = \langle f(\partial_x g) - (\partial_x f)g\rangle_1, \\
&[\langle f\rangle_2, \langle g\rangle_0] = 2\langle f(\partial_x g)\rangle_1, \\
&[\langle f\rangle_2, \langle g\rangle_1] = \langle 2f(\partial_x g) - (\partial_x f)g\rangle_2 - \tfrac{1}{2}\left\langle 2(\partial_x f)(\partial_x^2 g) + f(\partial_x^3 g)\right\rangle_0, \\
&[\langle f\rangle_2, \langle g\rangle_2] = 2\langle f(\partial_x g) - (\partial_x f)g\rangle_3 + \left\langle 2(\partial_x^2 f)(\partial_x g) - 2(\partial_x f)(\partial_x^2 g) + (\partial_x^3 f)g - f(\partial_x^3 g)\right\rangle_1, \\
&[\langle f\rangle_3, \langle g\rangle_0] = 3\langle f(\partial_x g)\rangle_2 - \tfrac{1}{2}\left\langle 3(\partial_x f)(\partial_x^2 g) + f(\partial_x^3 g)\right\rangle_0, \\
&[\langle f\rangle_4, \langle g\rangle_0] = 4\langle f(\partial_x g)\rangle_3 - 2\left\langle 3(\partial_x f)(\partial_x^2 g) + f(\partial_x^3 g)\right\rangle_1.
\end{aligned} \tag{A.1}$$

There is rich algebraic theory underlying these differential operators (Singh 2015), including a general formula for (A.1). In principle, however, the above rules can be verified by application of the chain rule.

Remark 11 *Note that, by definition (2.3),*

1. *these brackets are linear, so that* $\langle 2f(\partial_x g) - (\partial_x f)g\rangle_2 = 2\langle f(\partial_x g)\rangle_2 - \langle(\partial_x f)g\rangle_2$,
2. $\langle f\rangle_0 = f$; *and*
3. $\langle 1\rangle_2 = \partial_x^2$.

With this new notation in place and using (A.1), we can now simplify commutators using the terminology of anti-commutators,

$$\begin{aligned}
[\mathrm{i}\partial_x^2, \mathrm{i}V] &= -[\langle 1\rangle_2, \langle V\rangle_0] = -2\langle \partial_x V\rangle_1, \\
[\mathrm{i}V, [\mathrm{i}\partial_x^2, \mathrm{i}V]] &= -\mathrm{i}[\langle V\rangle_0, [\langle 1\rangle_2, \langle V\rangle_0]] = 2\mathrm{i}\left\langle (\partial_x V)^2\right\rangle_0, \\
[\mathrm{i}\partial_x^2, [\mathrm{i}\partial_x^2, \mathrm{i}V]] &= -\mathrm{i}[\langle 1\rangle_2, [\langle 1\rangle_2, \langle V\rangle_0]] = \mathrm{i}\left\langle \partial_x^4 V\right\rangle_0 - 4\mathrm{i}\left\langle \partial_x^2 V\right\rangle_2.
\end{aligned}$$

Straightforward discretisations of these operators preserve the symmetries that are crucial for retaining unitarity.

B Symmetric Zassenhaus splitting

The symmetric Zassenhaus splitting algorithm has crucial advantages over conventional splittings (Bader et al. 2014). It provides neat separation of terms with differing scales and structures, each of which is easy to exponentiate separately either on account of the structure or of the size. It achieves this separation by a recursive application of the symmetric *Baker–Campbell–Hausdorff formula* (usually known in an abbreviated form as the sBCH formula),

$$\mathrm{e}^{\frac{1}{2}X}\mathrm{e}^{Y}\mathrm{e}^{\frac{1}{2}X} = \mathrm{e}^{\mathrm{sBCH}(X,Y)}, \tag{B.1}$$

for X and Y in a Lie algebra $\mathfrak{g}$, where

$$\mathrm{sBCH}(hX, hY) = h(X+Y) - h^3(\tfrac{1}{24}[[Y,X],X] + \tfrac{1}{12}[[Y,X],Y]) + \mathcal{O}\left(h^5\right). \tag{B.2}$$

The expansion (B.2) features terms of the Hall basis (Reutenauer 1993), such as $[[Y,X],X]$ and $[[Y,X],Y]$, and can be computed to an arbitrary power of h using an algorithm from (Casas & Murua 2009). Coefficients and terms of the Hall basis for sufficiently high degree sBCH expansions are also available in a tabular form (Murua 2010). Since (B.1) is palindromic, only odd powers of h feature in the expansion (B.2).

For instance, consider the task of approximating $\mathrm{e}^{\mathcal{W}^{[0]}}$, where $\mathcal{W}^{[0]} = X + Y$, to an accuracy of $\mathcal{O}\left(h^5\right)$ under the assumption $X, Y = \mathcal{O}(h)$. Using the sBCH formula (B.1), and with the choice of $W^{[0]} = X$ as our first exponent, we write

$$\mathrm{e}^{\mathcal{W}^{[0]}} = \mathrm{e}^{\frac{1}{2}W^{[0]}}\mathrm{e}^{\mathrm{sBCH}(-W^{[0]},\mathcal{W}^{[0]})}\mathrm{e}^{\frac{1}{2}W^{[0]}}, \tag{B.3}$$

$$\begin{aligned}
\mathcal{W}^{[1]} := \mathrm{sBCH}(-X, X+Y) &= (-X + (X+Y)) - \tfrac{1}{24}[[X+Y,X],X] \\
&\quad + \tfrac{1}{12}[[X+Y,X],X+Y] + \mathcal{O}\left(h^5\right) \\
&= Y + \tfrac{1}{24}[[Y,X],X] + \tfrac{1}{12}[[Y,X],Y] + \mathcal{O}\left(h^5\right).
\end{aligned} \tag{B.4}$$

Note that $\mathcal{W}^{[1]} = Y + \mathcal{O}\left(h^3\right)$ and thus we have extracted $W^{[0]} = X$ from the exponent $\mathcal{W}^{[0]} = X + Y$ at the cost of correction terms in form of higher-order commutators $Z = \frac{1}{24}[[Y, X], X] + \frac{1}{12}[[Y, X], Y] = \mathcal{O}\left(h^3\right)$ appearing[6] in $\mathcal{W}^{[1]}$. At the next stage, we extract the largest term from $\mathcal{W}^{[1]} = Y + Z$, which is $W^{[1]} = Y = \mathcal{O}(h)$,

$$\mathrm{e}^{\mathcal{W}^{[1]}} = \mathrm{e}^{\frac{1}{2}W^{[1]}} \mathrm{e}^{\mathrm{sBCH}(-W^{[1]}, \mathcal{W}^{[1]})} \mathrm{e}^{\frac{1}{2}W^{[1]}}, \tag{B.5}$$

and $\mathcal{W}^{[2]} = \mathrm{sBCH}(-W^{[1]}, \mathcal{W}^{[1]}) = Z + \mathcal{O}\left(h^5\right)$ features grade three and higher commutators of Y and Z (or grade five and higher commutators of X and Y) as corrections, which can be discarded. Thus, by combining (B.3) and (B.5), the recursive algorithm terminates with the splitting

$$\exp(X + Y) = \mathrm{e}^{\frac{1}{2}W^{[0]}} \mathrm{e}^{\frac{1}{2}W^{[1]}} \mathrm{e}^{\mathcal{W}^{[2]}} \mathrm{e}^{\frac{1}{2}W^{[1]}} \mathrm{e}^{\frac{1}{2}W^{[0]}} + \mathcal{O}\left(h^5\right),$$

where $W^{[0]}$ and $W^{[1]}$ are $\mathcal{O}(h)$ and $\mathcal{W}^{[2]}$ is $\mathcal{O}\left(h^3\right)$. A sixth-order splitting would feature an additional exponent, $\mathcal{W}^{[3]} = \mathcal{O}\left(h^5\right)$. These exponential splittings are, thus, characterised by an expansion in increasing powers of the parameter h and we say that they are *asymptotic splittings* in h.

We emphasize that, in principle, we are free to choose the elements $W^{[k]}$ that we want to extract in each step of the algorithm,

$$\mathrm{e}^{\mathcal{W}^{[k]}} = \mathrm{e}^{\frac{1}{2}W^{[k]}} \mathrm{e}^{\mathcal{W}^{[k+1]}} \mathrm{e}^{\frac{1}{2}W^{[k]}}, \quad \mathcal{W}^{[k+1]} = \mathrm{sBCH}(-W^{[k]}, \mathcal{W}^{[k]}). \tag{B.6}$$

This choice can afford a great deal of flexibility – it could be based on some structural property which allows for trivial exponentiation of $W^{[k]}$ when extracted separately, a small spectral radius which makes the term amenable to effective exponentiation through Krylov subspace methods, a combination of both, or some other criteria. As long as the terms are decreasing in size, the convergence of the procedure is guaranteed. This can lead to many variants of the splitting, some of which could prove to have more favourable properties than others.

Analysing the sizes of terms in powers of h might seem natural in some cases such as ODEs but is not the only choice. In the case of the Schrödinger equation in the semiclassical regime, for instance, the semiclassical parameter ε is a more natural choice due to the considerations outlined in Subsection 2.2. In this case the exponents in a symmetric Zassenhaus splitting,

$$\exp(X + Y) = \mathrm{e}^{\frac{1}{2}W^{[0]}} \mathrm{e}^{\frac{1}{2}W^{[1]}} \cdots \mathrm{e}^{\frac{1}{2}W^{[s]}} \mathrm{e}^{\mathcal{W}^{[s+1]}} \mathrm{e}^{\frac{1}{2}W^{[s]}} \cdots \mathrm{e}^{\frac{1}{2}W^{[1]}} \mathrm{e}^{\frac{1}{2}W^{[0]}} + \mathcal{O}\left(\varepsilon^r\right),$$

are expanded in powers of ε.

[6]Since we are expanding to an accuracy of $\mathcal{O}\left(h^5\right)$, we can safely discard here all $\mathcal{O}\left(h^5\right)$ terms.